2012

SH-WAVE REFRACTION AND REFLECTION INVESTIGATION OF QUATERNARY GEOLOGY—CENTRAL UNITED STATES SEISMIC OBSERVATORY

Carrington L. Wright
University of Kentucky, carlwrig@hotmail.com

STUDENT AGREEMENT:

I represent that my thesis or dissertation and abstract are my original work. Proper attribution has been given to all outside sources. I understand that I am solely responsible for obtaining any needed copyright permissions. I have obtained and attached hereto needed written permission statements(s) from the owner(s) of each third-party copyrighted matter to be included in my work, allowing electronic distribution (if such use is not permitted by the fair use doctrine).

I hereby grant to The University of Kentucky and its agents the non-exclusive license to archive and make accessible my work in whole or in part in all forms of media, now or hereafter known. I agree that the document mentioned above may be made available immediately for worldwide access unless a preapproved embargo applies.

I retain all other ownership rights to the copyright of my work. I also retain the right to use in future works (such as articles or books) all or part of my work. I understand that I am free to register the copyright to my work.

REVIEW, APPROVAL AND ACCEPTANCE

The document mentioned above has been reviewed and accepted by the student's advisor, on behalf of the advisory committee, and by the Director of Graduate Studies (DGS), on behalf of the program; we verify that this is the final, approved version of the student's dissertation including all changes required by the advisory committee. The undersigned agree to abide by the statements above.

Carrington L. Wright, Student

Dr. Edward Woolery, Major Professor

Dr. Alan Fryar, Director of Graduate Studies

SH-WAVE REFRACTION AND REFLECTION INVESTIGATION OF QUATERNARY GEOLOGY—CENTRAL UNITED STATES SEISMIC OBSERVATORY

THESIS

A thesis submitted in partial fulfillment of the
requirements for the degree of Master of Science in the
College of Arts and Sciences
at the University of Kentucky

By

Carrington L. Wright

Lexington, Kentucky

Director: Dr. Edward W. Woolery, Associate Professor of Geophysics

Lexington, Kentucky

2012

ABSTRACT OF THESIS

SH-WAVE REFRACTION AND REFLECTION INVESTIGATION OF QUATERNARY GEOLOGY—CENTRAL UNITED STATES SEISMIC OBSERVATORY

The Central United States Seismic Observatory (CUSSO) consists of an array of vertical strong motion accelerometers and medium period seismometers that penetrate 585 m into the Mississippi Embayment sediments and terminates into Paleozoic bedrock. The array is located in the New Madrid Seismic Zone within the upper embayment. The thick unconsolidated Quaternary sediments have the potential to influence strong motions; understanding how these sediments affect ground motion is the goal of the CUSSO array. Nine SH-wave refraction and five P-wave common midpoint reflection surveys were collected within a 1 km radius around the CUSSO borehole in order to characterize the local seismic stratigraphy. Three major seismic boundaries from SH-wave refraction and six P-wave continuous reflection boundaries were interpreted. Combined, both methods were used to characterize seismic horizons (Quaternary to Paleozoic) around the CUSSO in terms of velocity and depth. Faults in the area are subparallel and northeast-southwest trending. Some faults appear to deform Eocene and Quaternary sediments, although no surface expression has been found.

KEYWORDS: New Madrid Seismic Zone, Central United States Seismic Observatory, Quaternary, Velocity Models, Near Surface

Carrington L. Wright

September 2012

SH-WAVE SEISMIC REFRACTION AND REFLECTION INVESTIGATION OF QUATERNARY GEOLOGY—CENTRAL UNITED STATES SEISMIC OBSERVATORY

By
Carrington L. Wright

Edward W. Woolery
Director of Thesis

Alan E. Fryar
Director of Graduate Studies

September 2012

TABLE OF CONTENTS

TABLE OF CONTENTS IV
LIST OF FIGURES VI
LIST OF TABLES VII
LIST OF EQUATIONS VIII
CHAPTER ONE: INTRODUCTION 1
1.1 Problem 1
1.2 Previous Work 2
1.3 Specific Tasks and Objectives 3
1.4 Regional Geology 3
1.5 Field Location 6
1.6 Site Stratigraphy 7
1.7 CUSSO Borehole 9
CHAPTER TWO: METHODOLOGY 20
2.1 Seismic Refraction 20
2.1.1 Refraction Acquisition 20
2.1.2 Seismic-Refraction Processing 21
2.2 Refraction Inversion Method 24
2.2.1 Time-Term Inversion 24
2.3 Seismic Reflection 24
2.3.1 Seismic Reflection Acquisition 24
2.3.2 Seismic-Reflection Processing 25
2.4 Seismic Resolution 26
2.4.1 Seismic Reflection and Refraction Resolution 26
CHAPTER THREE: REFRACTION MODELS 40
3.1 Final CUSSO Refraction Lines 40
3.1.1 Four-Meter CUSSO 1 Refraction Line 40
3.1.2 Four-Meter CUSSO 2 Refraction Line 40
3.1.3 Four Meter CUSSO Four Refraction Line 41
3.1.4 Four-Meter CUSSO 5 Refraction Line 41
3.1.5 Four-Meter CUSSO 6 Refraction Line 42
3.1.6 Four Meter Full Refraction Survey Results 42

3.2 Sounding Tests 42
3.2.1 Two-Meter CUSSO 2 Sounding 43
3.2.2 Two-Meter CUSSO 4 Sounding 43
3.2.3 Two-Meter CUSSO Sounding Results 43
3.2.4 Four-Meter CUSSO 3 Sounding 44
3.2.5 Four-Meter CUSSO 4 Sounding 44
3.2.6 Four-Meter CUSSO Sounding Results 44
CHAPTER FOUR: SEISMIC REFLECTION 49
4.1 CUSSO Reflection Analysis 49
4.2 Fault Zone Interpretations 50
4.3 CUSSO 4 Fault Interpretation 51
CHAPTER FIVE: VELOCITY MAPS 62
5.1 Velocity Contour Maps 62
CHAPTER SIX: DISCUSSION 64
CHAPTER SEVEN: CONCLUSIONS 66
APPENDICES 69
APPENDIX A 69
APPENDIX B 82
APPENDIX C 87
BIBLIOGRAPHY 89
VITA 94

LIST OF FIGURES

Figure 1.1, The placement of the CUSSO accelerometers and seismometers.....11
Figure 1.2, The Kentucky Seismic and Strong-Motion Network. 12
Figure 1.3, Selected tectonic provinces of the central and eastern United States.....13
Figure 1.4, Geologic features surrounding the CUSSO.....14
Figure 1.5, Locations of seismic profiles. 15
Figure 1.6, Stratigraphic and gamma-ray log interpretations.. 16
Figure 1.7, The components of the OYO P-S logging system.....17
Figure 1.8, Results of the shear and compression P-S suspension tool 18
Figure 1.9, The 12 major impedance boundaries from the SH- and P-wave suspension logging tool. 19
Figure 2.1, The typical set-up for shear-wave refraction acquisition. 31
Figure 2.2, Three steps in the refraction process. 33
Figure 2.3, SH-Wave processing images. 35
Figure 2.4, P-Wave processing images. 36
Figure 3.1, Four-meter final refraction surveys.. 46
Figure 3.2, Refraction results from full four meter lines. 47
Figure 3.3, Two- and 4-meter CUSSO soundings. 48
Figure 4.1, The reinterpretation of the CUSSO 1 line.. 52
Figure 4.2, Reinterpretation of the CUSSO 2 line.. 53
Figure 4.3, Reinterpretation of the CUSSO 3 line. 54
Figure 4.4, Reinterpretation of the CUSSO 4 line.. 55
Figure 4.5, CUSSO 1 fault interpretations… 57
Figure 4.6, CUSSO 2 fault interpretation.. 58
Figure 4.7, CUSSO 3 fault interpretations.. 59
Figure 4.8, CUSSO 4 fault interpretations.. 60
Figure 4.9, Uninterpreted and interpreted deformation zone along CUSSO 4.. 61
Figure 5.1, Velocity structure contours at 10, 30, and 50 m depths.. 63
Figure 7.1, Major seismic intervals and velocities associated with the three models.. 68

LIST OF TABLES

Table 2.1, Acquisition parameters for 4 meter CUSSO full refraction lines. 29
Table 2.2, Acquisition parameters for refraction sounding tests. 30
Table 2.3, Geometry parameters.. 32
Table 2.4, Acquisition properties for CUSSO 4 SH-wave reflection 34
Table 2.5, The general P- and SH-wave reflection survey reprocessing procedures. 37
Table 4.1, The seismic two-way travel times from reinterpreted CUSSO data. 56

LIST OF EQUATIONS

Equation 2.1, Slope equation used in refraction analysis 23
Equation 2.2, $_{1/4}$ wavelength equation 27
Equation 2.3, $_{1/8}$ wavelength equation 27
Equation 2.4, Radius of first Fresnel Zone 27

CHAPTER ONE: INTRODUCTION

1.1 Problem

Historically, the New Madrid Seismic Zone has been linked with major earthquake activity in the central United States since the three major earthquakes of 1811 and 1812, (Braile et al. 1986) and it has had a major effect on nearly 5 million km^2 in the eastern United States (Bolt, 2003). The majority of the earthquakes that occur in this seismic zone occur within the Precambrian and lower Paleozoic strata at depths between 4 and 12 km beneath the northern part of the Mississippi Embayment (Van Arsdale and TenBrink, 2000). The New Madrid Seismic Zone has been the most active seismic source zone in the central and eastern United States and dominates the seismic hazard for much of the region (Bolt, 2003). The University of Kentucky's seismic network has recorded several hundred events with magnitudes between 1.5 and 5.2 in the seismic zone since the early 1990's (Wang and Woolery, 2006).

The New Madrid Seismic Zone (NMSZ) lies within the northern portion of the Mississippi Embayment. The embayment is a broad northeast-southwest-oriented trough, filled with as much as 1 km (near Memphis, Tenn.) of unlithified and poorly lithified clastic sediments, overlying carbonate Paleozoic bedrock. This thick sediment overburden can have a significant influence on ground-motion characteristics (such as amplitude, frequency, and duration). Understanding how strong ground motions are affected by thick layers of loosely consolidated sediment is a primary goal for the Central United States Seismic Observatory (CUSSO). CUSSO, located adjacent to the central segment of the NMSZ in Fulton County, Kentucky, is an array of vertical strong-motion accelerometers and medium-period seismometers (0.06–50 Hz) that penetrate the 585-

thick embayment sediments and terminate 8 m into the Paleozoic bedrock (Figure 1.1). In order to effectively model the transfer of the strong motion through the sediment at CUSSO, the subsurface geology at the site must be defined.

1.2 Previous Work

A previous study by Hunter (2011) collected P-wave reflection data within a 1-km^2 area surrounding the CUSSO location in order to determine the elevation, geometry, and dynamic properties of the major impedance horizons. That study consisted of four reflection profiles, which interpreted four major subsurface impedance boundaries, designated zones 2-5. These zones represent the tops of the site's deeper stratigraphic horizons (i.e., Paleocene, Cretaceous and Paleozoic). Hunter (2011) did not assign a zone 1 because the aperture of his acquisition array precluded him from sampling the uppermost (or Quaternary) sediment. His zone 2 was found at an average depth of 290 m and corresponded to the Eocene Wilcox Formation. Zone 3 was at approximately 400 m and was interpreted to be the Paleocene Porters Creek Formation. Zone 4, at 490 m, was interpreted as being the Cretaceous McNairy Formation, and the deepest seismic horizon in Hunter's (2011) work was the Paleozoic bedrock at 590 m. Three high-angle faults were also imaged in his study. These faults were interpreted to extend from Paleozoic bedrock to the Cretaceous McNairy Formation, and in some cases extending into the Eocene and Paleocene. This study reprocessed the Hunter (2011) P-wave lines using newly acquired signal-processing software in order to better define these primary reflectors; however, the primary objective of this investigation is to use SH-wave refraction and reflection methods to characterize the elevation, geometry, and dynamic properties of significant impedance horizons within the previously unsampled Quaternary

sediment. Part of this process was acquiring reflection data over a fault interpreted by Hunter (2011), in order to determine if it extended into the Quaternary sediment.

1.3 Specific Tasks and Objectives

In order for realistic, high-resolution ground-motion response models to be constructed for the CUSSO site, an accurate geometric and dynamic characterization of the significant geologic horizons must be performed. Previous studies successfully characterized the deeper Tertiary to Paleozoic horizons, but none have successfully characterized the near-surface Quaternary sediment. Consequently, SH-wave seismic refraction and reflection surveys were undertaken to define the dynamic and geometric configuration of the shallow Quaternary sediment. The specific tasks and goals were:

a) Collect SH-wave refraction data coincident with previous P-wave surveys to generate seismic velocities and depths/elevations for the major impedance intervals within the Quaternary stratigraphic section.

b) Acquire a near-surface SH-wave seismic-reflection image coincident with the location of an interpreted fault on the Hunter (2011) P-wave survey in order to assess the near-surface extent of the deformation.

c) Integrate the Quaternary seismic intervals with the previously defined Tertiary-Paleozoic intervals to construct a complete velocity model for the CUSSO site. This task includes reprocessing previous P-wave lines using newly acquired signal-processing software that has more robust filtering algorithms than previously available software.

1.4 Regional Geology

The Central United States Seismic Observatory (CUSSO) site in Sassafras Ridge, Ky., is one of nine stations in the state that exclusively monitor strong ground motion

(Figure 1.2). It is one of four stations that are vertically arrayed, and one of two vertical arrays that have a bedrock accelerometer. The CUSSO is the only vertical array in the central United States to have penetrated and instrumented the thick Mississippi Embayment sediment, and one of two of its kind in the nation to measure ground-motion response in deep sediments (E. Woolery, personal communication). The CUSSO site is located in the northern Mississippi Embayment and is situated on approximately 585 m of marine and fluvial sediments that overlie bedrock. The ancillary borehole terminates approximately 10 m into Paleozoic bedrock. The Mississippi Embayment lies within the Eastern Granite-Rhyolite Tectonic Province (Figure 1.3). The Mesoproterozoic Eastern Granite-Rhyolite Tectonic Province is part of the larger Precambrian North American craton, which is a collection of multiple tectonic terranes, that formed by lateral accretion to the continental crust prior to approximately 1600 Ma (Heigold and Kolata 1993). This province can be split between the eastern and southern sections that formed between 1470 and 1370 Ma, respectively (Van Schmus, et al., 1996) and consists of A-type granitic and rhyolitic rocks. These types of rocks are commonly connected to continental extension or rifting (Slagstad, et al., 2009).

During the late Proterozoic, the embayment was affected by the breakup of Rodinia and the subsequent opening of the Iapetus Ocean. This initiated the formation of a large northeast-oriented graben system. This graben system is often divided into three main segments: the Reelfoot Rift, Rough Creek Graben, and Rome Trough. The Reelfoot Rift has been described in aeromagnetic and gravity surveys (see, for example Kane et al., 1981) as a northeast-trending basement depression 70 x 300 km long, that extends from the southern cratonic margin into the Eastern Granite-Rhyolite Province (Soderberg

and Keller, 1981; Keller et al., 1983; Drahovzal et al., 1992). The east-west-oriented Rough Creek Graben (Figure 1.4) is located in western Kentucky and is bounded by the Rough Creek-Shawneetown fault system to the north and by the Pennyrile fault system to the south (Woolery, et al., 2003).

The Rough Creek-Shawneetown Fault System extends west from Kentucky into southern Illinois and then joins the northeast-trending Lusk Creek and Raum Fault Zones. This collection of faults forms the northwestern border of the Fluorspar Area Fault Complex (Nelson and Lumm, 1985). The Rough Creek Graben and the Reelfoot Rift formed as part of the larger Mississippi River Graben System (Thomas, 1976, 1983, and 2006); however, the relationship between these two structures is still debated. Howe and Thomas (1985) suggested that the Reelfoot Rift and the Rough Creek Graben were related structures, whereas Kolata and Nelson (1991) considered the Rough Creek Graben to be the east-west continuation of the Reelfoot Rift. The formation of the Reelfoot Rift was proposed (Kane et al, 1981; Hildenbrand 1985; Hendricks 1988; Nelson and Zhang, 1991; Dart and Swolfs, 1998) to have formed along the boundary in the middle of adjacent terranes, underneath the Eastern section of the Granite-Rhyolite Province. Another possible mechanism to explain the Reelfoot rifting could have been a mantle plume upwelling along terrane boundaries (Dart and Swolfs, 1998). An alternate explanation (Thomas, 1985, 1991) suggests the Reelfoot Rift is the result a network of right-lateral strike-slip motion along a northwest-southeast-striking transform fault.

The Mississippi Embayment is in the Eastern Granite-Rhyolite Province (EGRP). The province is bounded by the Central Plains Orogen, the Penokean Orogen, the Midcontinent Rift System to the north, the Mesoproterozoic Grenville Orogen to the east,

and the late Precambrian cratonic margin along the southern margin (Tollo et al., 2004). Van Arsdale (2009) described the embayment as a broad, shallow, south-plunging trough filled with unlithified sands, silts, marls, and clays that were deposited during the subsidence and ingress of the ancient Gulf of Mexico.

The traditional explanation for the formation of the Mississippi Embayment is that a large graben system, in which the embayment sits, called the Mississippi Valley Graben Fault System, was reactivated and later subsided during the opening of the Gulf of Mexico. This allowed a northernly opening for the entrance of the Gulf of Mexico to form during the Late Cretaceous (Braile et al., 1986; Ervin and McGinnis, 1975). Cox and Van Arsdale (1997, 2002) proposed that the Mississippi Embayment formed as the area drifted over the Bermuda hot spot during the Cretaceous and that the thermally uplifted region created an arch, in which nearly 2 km of Paleozoic strata were eroded during the mid-Cretaceous (Cox and Van Arsdale, 1997). The movement off the hotspot during the late Cretaceous allowed for the remnant arch to cool and subside, forming the Mississippi Embayment trough (Csontos et al., 2008). The Late Cretaceous and Cenozoic sediment that filled the trough include the McNairy, Clayton, Porters Creek, Fort Pillow, Flour Island, Claiborne Group, Upland Complex, and the Mississippi River sediments (Howe and Thompson, 1984; Thomas, 1985).

1.5 Field Location

The study area is located in Fulton County in southwestern Kentucky (N36.551944, W89.329444). Locations of the six seismic refraction/reflection lines collected around the CUSSO borehole are shown in Figure 1.5. The two north-south lines are CUSSO 1 (Sassafras Church Road) and CUSSO 2 (Running Slough Road). The two

east-west-oriented lines are CUSSO 3 (Chesshire Lane) and CUSSO 4 (State Highway 971). CUSSO 5 (Highway 94) is a north-south-oriented profile coincident with the borehole and between surveys 4 and 5. CUSSO 6 (Cotton Gin Road) is an east-west continuation of CUSSO 4.

1.6 Site Stratigraphy

The Mississippi Embayment is characterized by a south-plunging synclinal trough with dipping post-Paleozoic sediments that thicken to the south. The total depth to Paleozoic bedrock as defined by the CUSSO borehole is approximately 585 m. Prior to setting the borehole casing, downhole resistivity, gamma-ray, and sonic velocity (P- and S-wave) logs were acquired and used along with borehole cuttings to distinguish the lithologic boundaries. Together, the borehole geophysical logs and sample descriptions (Figure 1.6.) provided generalized stratigraphic interpretations for the CUSSO site.

There is 48 m of surficial Quaternary alluvium above the Eocene Jackson Formation; the majority of these sediments are fine and coarse sands. The contact between the Quaternary sediments and the Jackson Formation represents a change between upper coarse sands and gravel and underlying black clay.

The Jackson Formation is an unlithified Eocene silty clay unit (Woolery et al., 1993). It can contain fine and coarse sand facies, but is mainly silty clay. The silt and clay are olive gray to light green and light gray to black and are very sandy and micaceous (Olive, 1972). The sand is medium gray to light gray to brown and weathers yellowish orange to reddish (Olive, 1980) and is composed of fine to very coarse grains. The sand intervals vary between thin and thick bedding with common crossbedding and cut-fill structures that represent river and lake deposits. Palynomorph assemblages are also

present in this formation, possibly representing a continental lacustrine depositional environment, but marine assemblages have been found in some localities (Olive, 1980).

The boundary between the Eocene Jackson and underlying lower Eocene Claiborne Formations is approximately 131 m below the surface elevation. This assemblage is composed of primarily medium-to very fine-grained sands, silts, and clays of nonmarine origin, although some marine intervals have been found (Conrad, 1847). The sands range from light to dark gray, white, brown, and red depending on weathering. The silts and clays are light to dark gray, whereas intervals with carbonaceous material tend to be dark brown to black. Silts have higher clay content, and the clays are normally more silty or sandy. Lignite beds are also found in this interval. The Claiborne is subdivided into the Carrizo Sand, Cane River Formation, Sparta Sand, Cook Mountain Formation, Cockfield Formation, and the Memphis Sand. The lower contact is thought to be unconformable with the Wilcox Group and, although the borehole thickness is approximately 180 m, various localities may have thicknesses as much as 450 m (Conrad, 1847; Hilgard, 1860).

The boundary that separates the Claiborne Formation and the Wilcox Group is at approximately 274 m. The Wilcox Group was described by Crider and Johnson (1906) as nonmarine sands, silts, clays, and gravels; some lignite is found at various locations. Sands are fine to very fine grained, and both sands and clays are light gray or brown; clays are often sandy and silty. The inclusion of carbonate material results in dark brown to black colors. The lignite in the sequence is controlled by depositional environments and not stratigraphy, and it is not found in the CUSSO borehole.

Below the Wilcox, the Midway Group consists of the Porters Creek Clay and Fort Pillow Formation. The Fort Pillow Formation is made up mostly of sands with pyrite, lignite, and chert. The Porters Creek lies unconformably below the Wilcox Formation and is composed of dark gray clay; sections of glauconitic sands are common in the upper and lower parts of the clay (Olive, 1972). Because of high clay content, this formation is known to shrink and swell (Easson et al., 2005).

The McNairy Formation is a loose to friable sand with interbedded clays, micas, and silts; it was determined to be a part of a deltaic system during the Cretaceous Period (Pryor, 1960). Below the Cretaceous sediments, at approximately 585 m, is the boundary between the Cretaceous and underlying Paleozoic carbonate bedrock.

1.7 CUSSO Borehole

The geophysical borehole data were collected between September and October of 2006 by GeoVision Geophysical Services in order to determine the stratigraphy, as well as seismic shear and compression wave velocities for the CUSSO site. To determine the average velocity of the sediment column surrounding the boring, the P-S Logging System was used (Figure 1.7). The P-S suspension probe system is made up of a reversible-polarity solenoid, horizontal-shear wave, and compression-wave source that are connected to two biaxial receivers by a cylinder. The receivers are separated by 1 m and this separation allows for an average velocity calculation to be made by inversion of travel time between receivers (GeoVision Geophysical Services, 2007). The source and receiver probe are suspended in the boring via a cable that relays signals from the probe receivers to instrumentation on the surface. The connection cable is also used to measure depth of the probe while it is in the boring. The source is not coupled directly to the

boring walls, creating a horizontal pressure wave within the boring. Once the pressure wave passes through the surrounding sediment and boring casing it is converted into P- and S-waves.

In general, this process is conducted in three steps. First, the source is generated in one direction, creating a horizontal shear wave at the same time the horizontal receivers are situated parallel to the axis of motion. Next, the source is generated again in an opposite direction while the receivers remain in the previous orientation; this is done to change the polarity. Finally, the source is generated and the vertical receiver records the signal. By repeating this process over several iterations, a stronger signal can be created. The suspension velocity log was collected in an uncased fluid-filled boring that was drilled with rotary mud. Individual P- and S-wave velocity measurements are reliable over the 1-m collection interval (Figure 1.8). In the case of the CUSSO borehole, because of the diameter of the bore and background vibration, the precision of the velocity data is around 10 percent (GeoVision Geophysical Services, 2007). The P-and S-wave velocities generated from the suspension log derived 12 significant impedance boundaries (Figure 1.9).

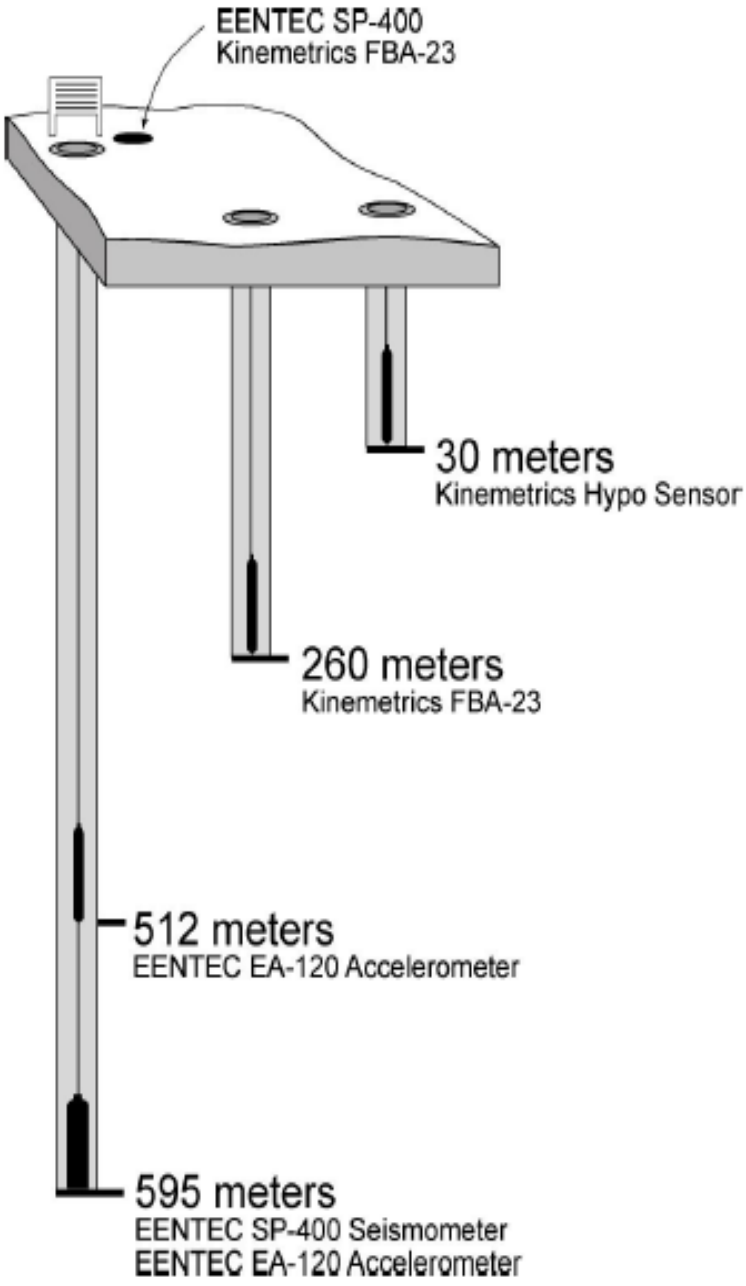

Figure 1.1. The placement of the CUSSO accelerometers and seismometers used to measure strong motion.

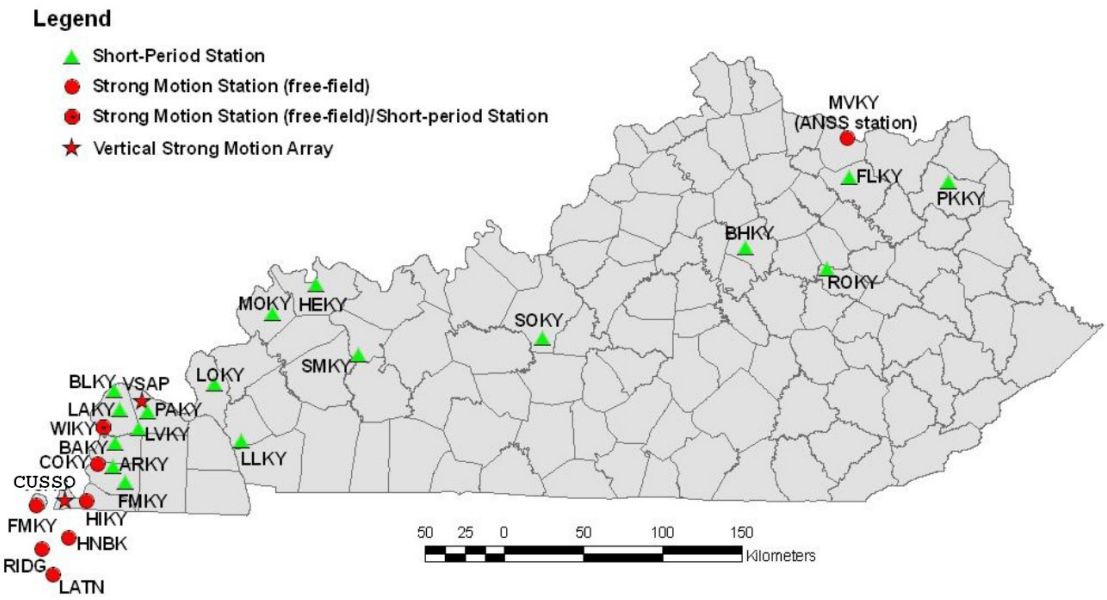

Figure 1.2. The Kentucky Seismic and Strong-Motion Network (KSSMN) operated by the University of Kentucky (http://www.uky.edu/KGS/geologichazards/equake3.htm).

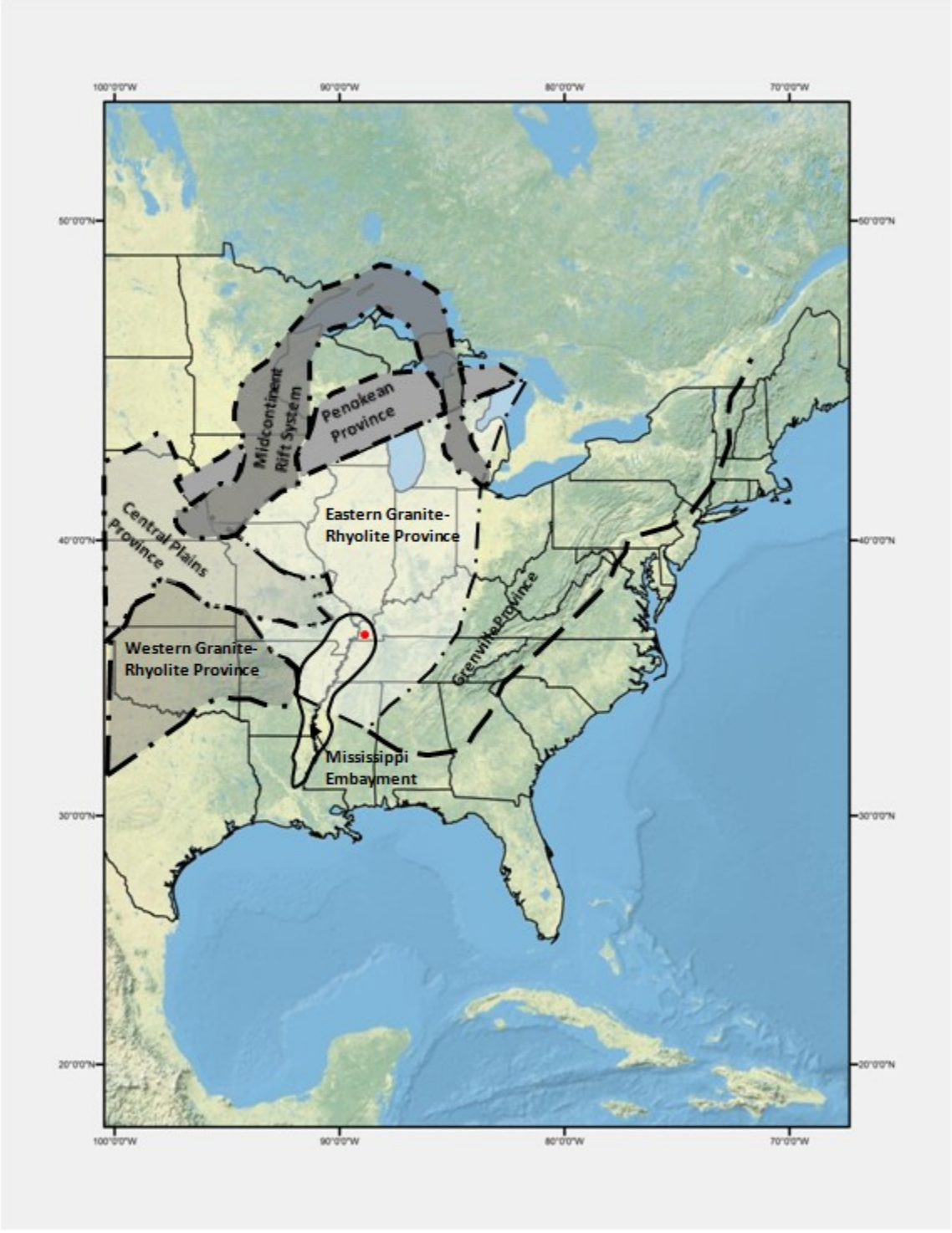

Figure 1.3. Selected tectonic provinces of the central and eastern United States (after Bickford et al., 1986).

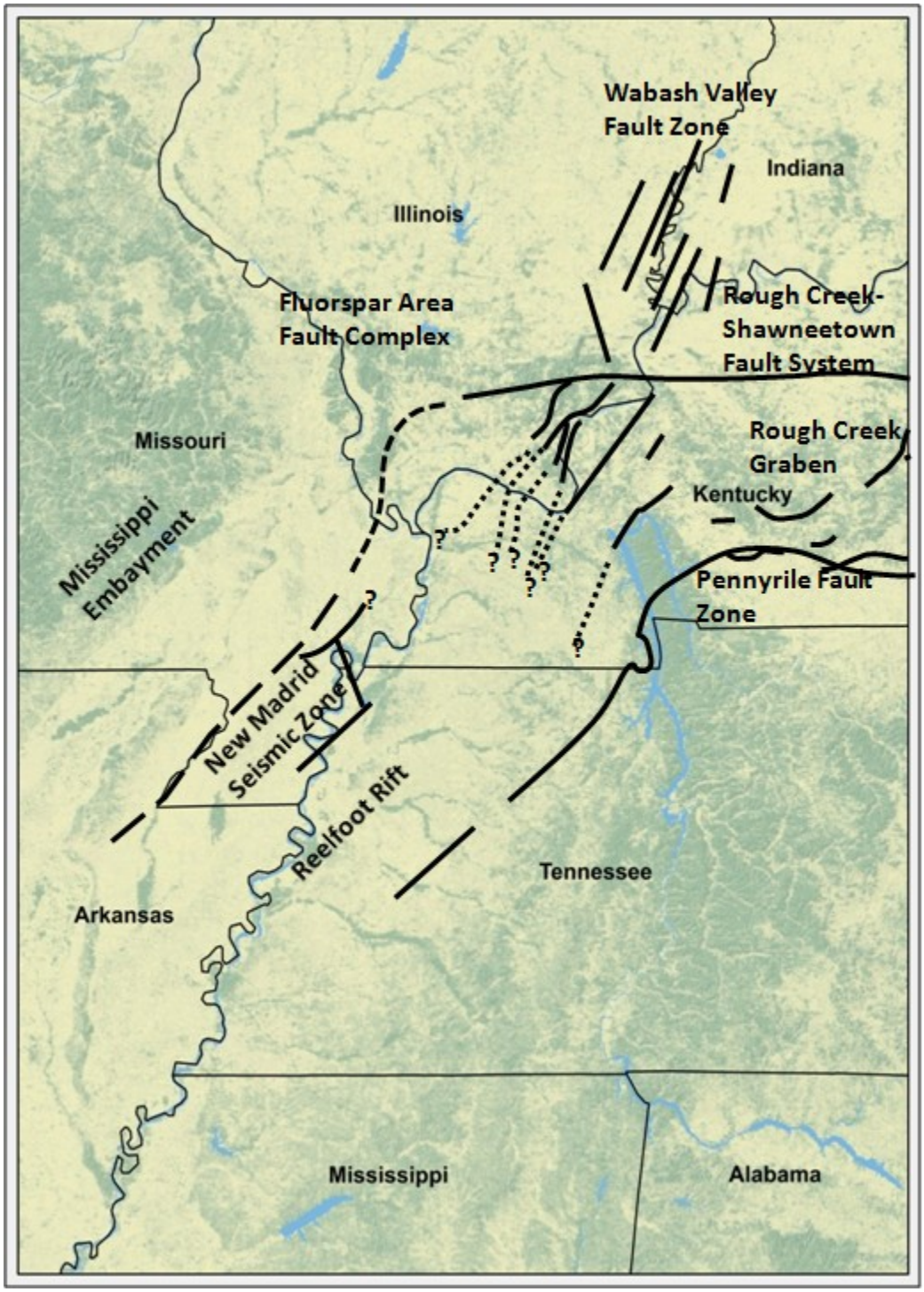

Figure 1.4. Geologic features surrounding the Central United States Seismic Observatory (red box) (modified from Kolata and Nelson, 1991).

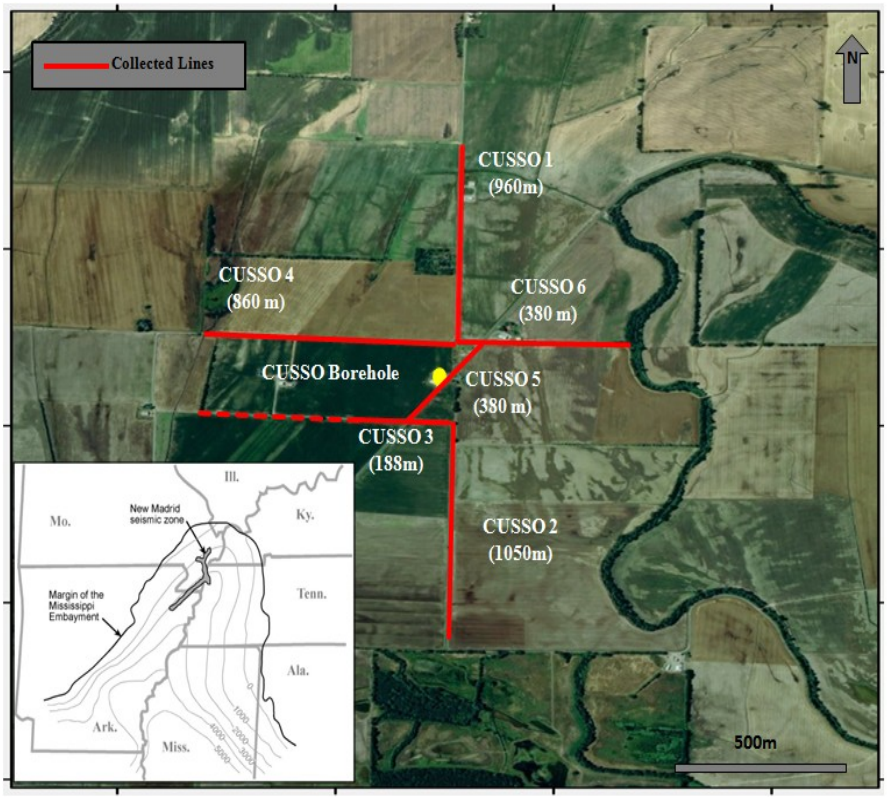

Figure 1.5. Locations of seismic profiles. The CUSSO borehole is in the center (red circle). The red lines are the refraction/reflection lines that run along roads surrounding the CUSSO borehole.

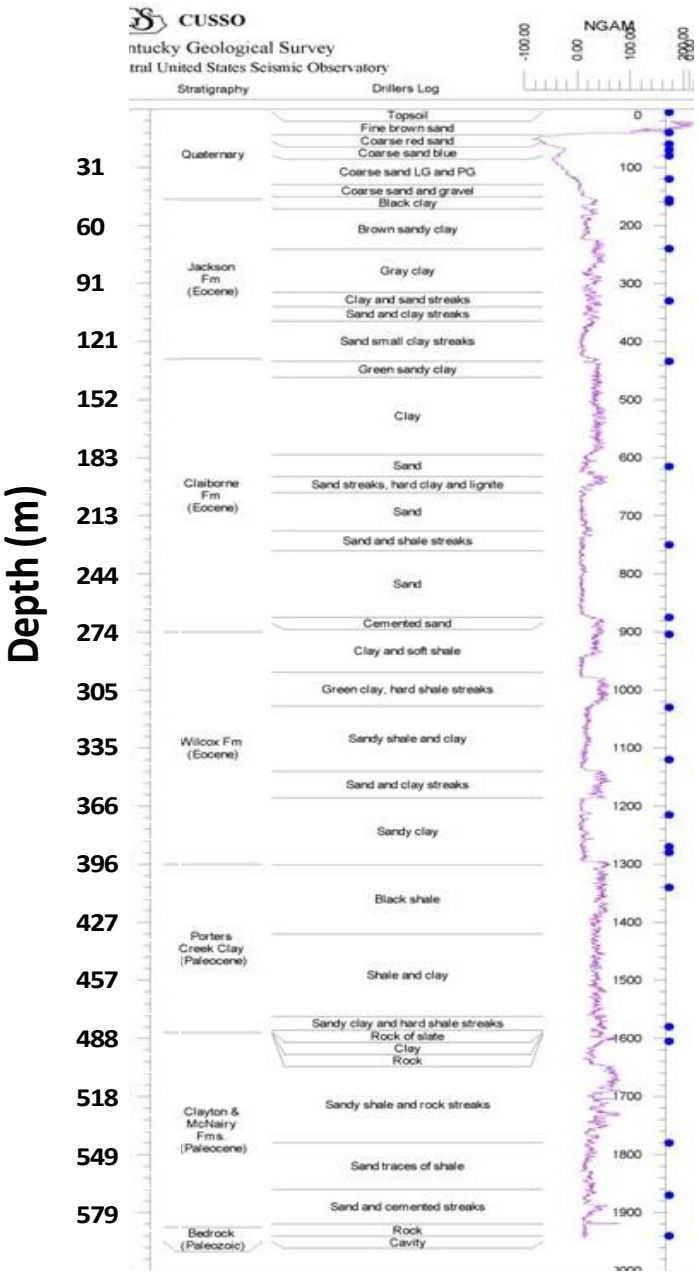

Figure 1.6. Stratigraphic and gamma-ray log interpretations from the CUSSO borehole. Stratigraphy was interpreted from cuttings collected at the borehole by Steve Martin, Kentucky Geological Survey.

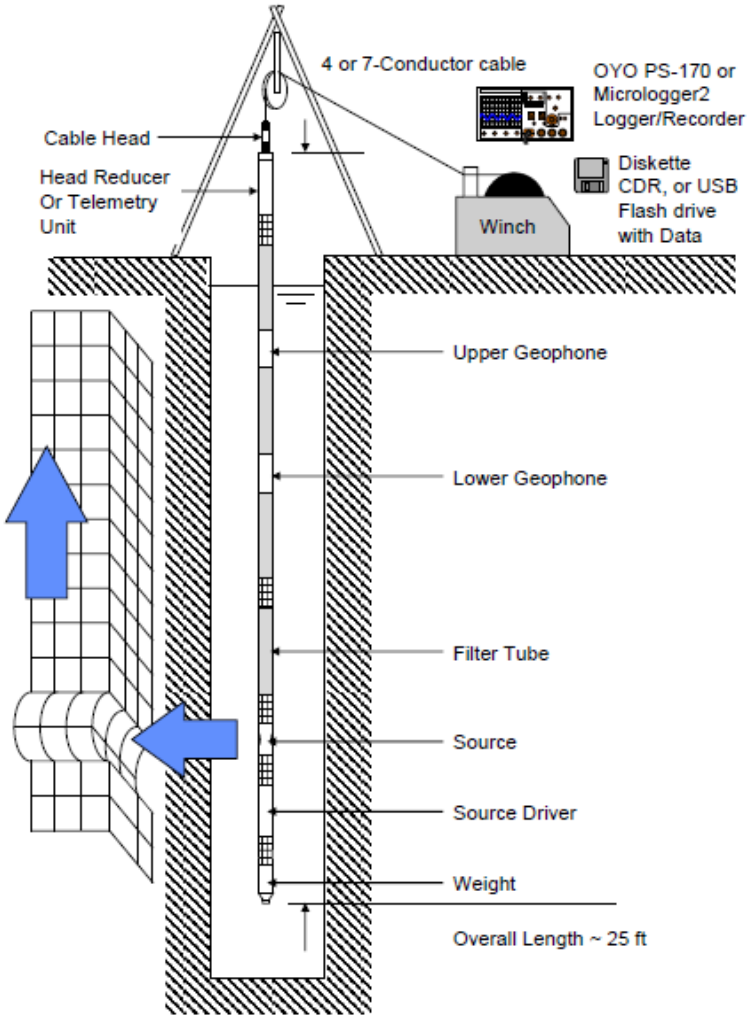

Figure 1.7. The components of the OYO P-S logging system used in the velocity analysis of the CUSSO borehole (GeoVision Geophysical Services, 2007).

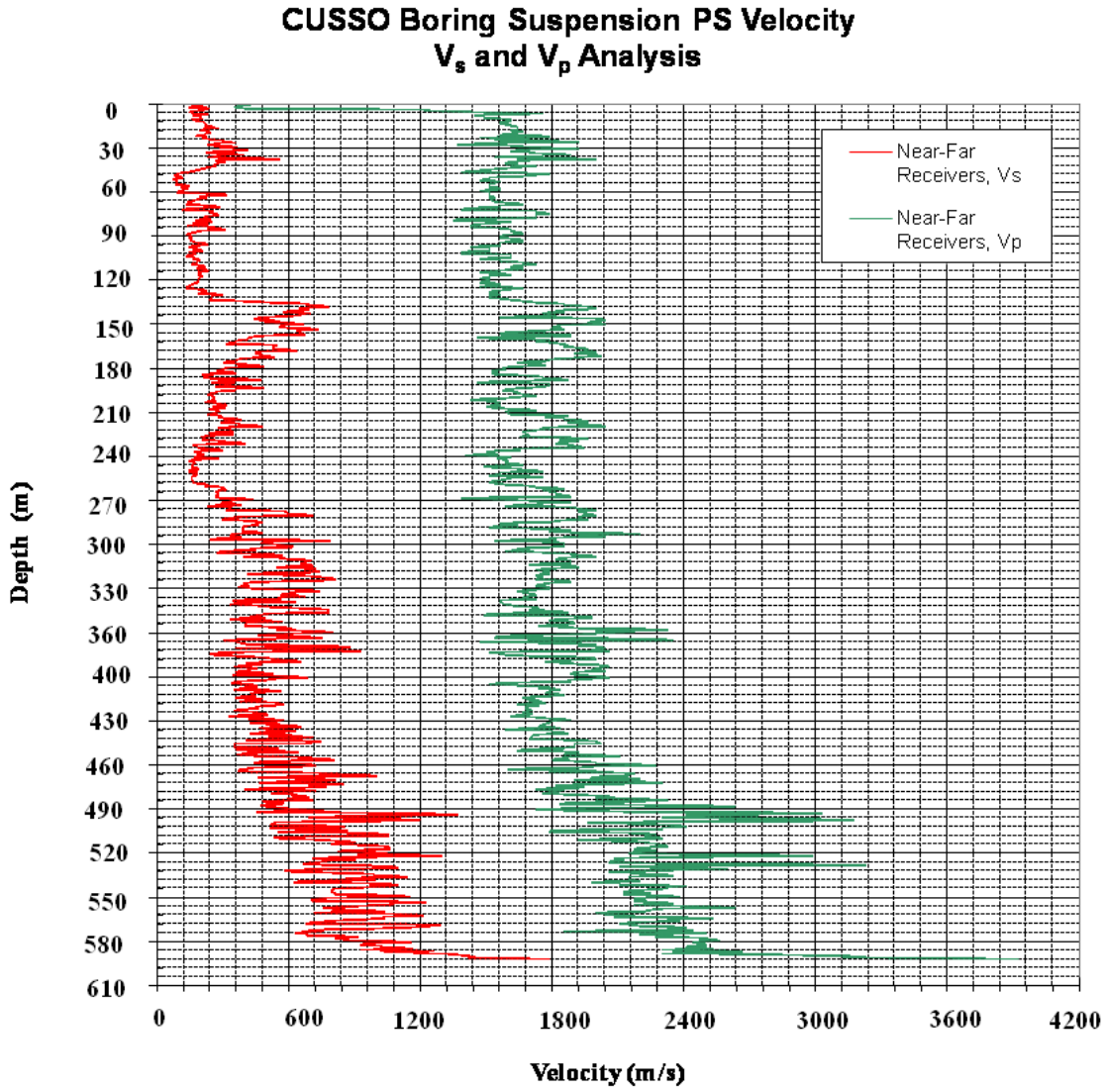

Figure 1.8. Results of the shear (vs) and compression (vp) P-S suspension tool (GeoVision Geophysical Services, 2007).

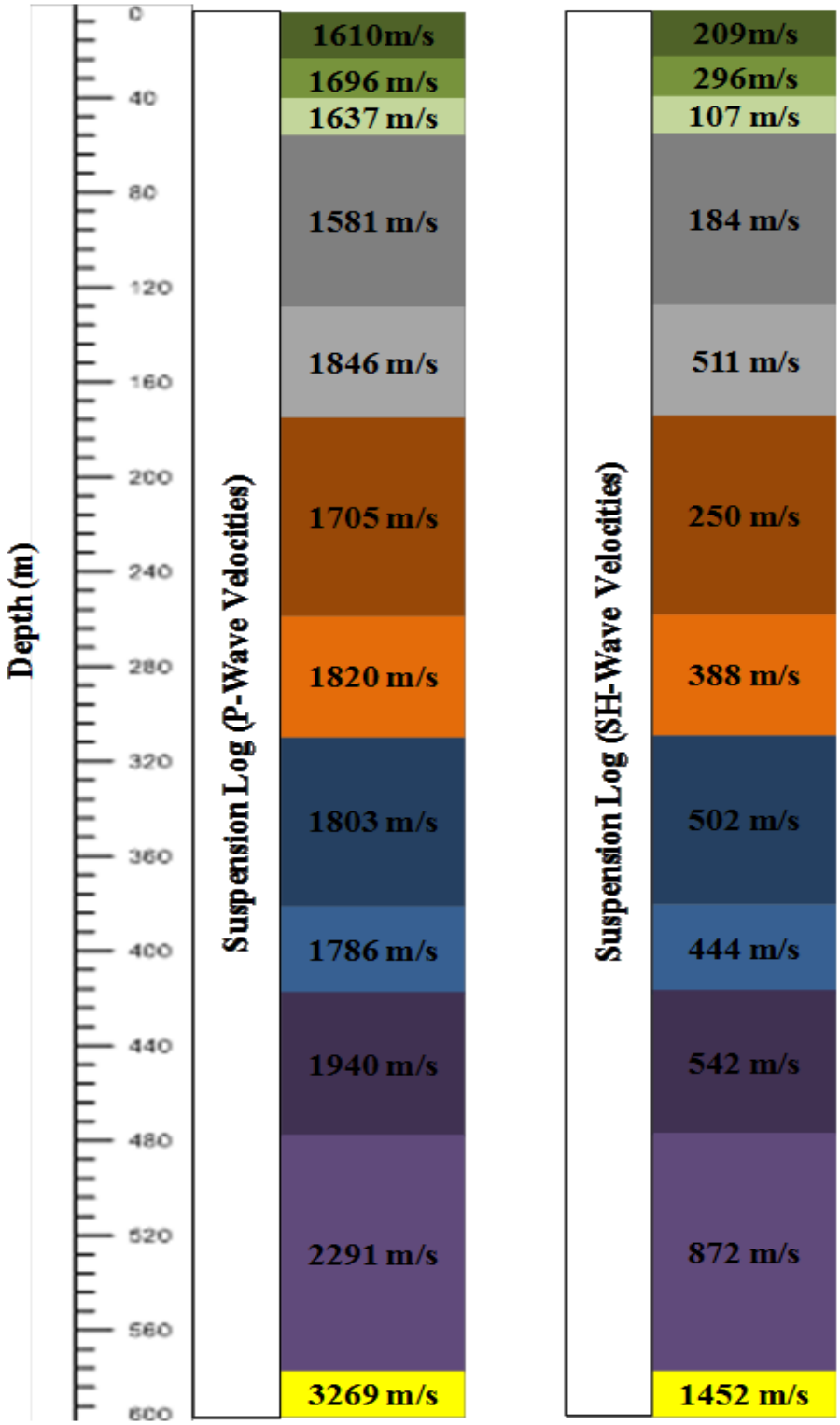

Figure 1.9. The 12 major impedance boundaries from the SH- and P-wave suspension logging tool.

CHAPTER TWO: METHODOLOGY

2.1 Seismic Refraction

2.1.1 Refraction Acquisition

A 48-channel Geometrics StrataVisor seismograph was used to collect the seismic refraction data. The seismograph has a dynamic range of 120db and stores data on an internal hard drive. The seismograph has two takeout cables to connect geophones. The cables have 24 takeouts each, allowing for a maximum of 48 geophones to be connected at one time. Two different types of geophones were used for collecting seismic-refraction data. Tables 2.1 and 2.2 outline detailed acquisition parameters for the refraction lines in this study.

Primarily, 30 Hz SH-wave geophones were used. The SH-wave geophones are horizontally polarized, leveled, and oriented in the same direction and orthogonal to the direction, of wave propagation during acquisition. Vertically polarized 40-Hz P-wave geophones were used during the initial source testing, but were not used for production acquisition. The seismic shear and compression waves were generated using 4-lb and 10-lb hammers. The hammers struck against a 6 x 6 in. hardened aluminum plate for P-wave acquisition and steel H-pile for SH-wave production surveys. For SH-wave surveys, the geophones are aligned parallel to the direction of the hammer swing and perpendicular to the direction of wave propagation (Figure 2.1). In order to enhance the first-arrival signal, multiple stacks (or hammer blows) were made at each shotpoint. In order to minimize P-wave contamination, the acquisition polarity was changed 180° on the seismograph and the direction of the hammer swing, thus constructively interfering with SH-wave generation and destructively interfering with any inadvertent P-waves.

During most of the refraction acquisition, a roll-along was needed. A roll-along is done by laying out 48-channel geophones and collecting the data at specific geophones, usually 1, 12, 24, 36, 48, and offsets, if needed. After the initial line is collected, the first 24 geophones are picked up and moved ahead of the remaining 24 geophones. An example of the geometric parameters for a multiple roll-along line is shown in (Table 2.3). Using a roll-along for seismic-refraction acquisition allows a profile to be constructed beyond the initial dimensions of the source and cable length. The roll-along of only the lead cable allows for overlap and redundancy in the subsurface source-to-receiver ray-path coverage, which is important for reducing residual error of the continuous velocity model (Chiemeke and Osazuwa, 2009).

2.1.2 Seismic-Refraction Processing

Refraction models were created using two programs within the SeisImager software suite. Pickwin version 4.2.0.0 picks first arrivals and dispersion curves. Plotrefa 2.9.1.9 was used for refraction velocity analyses. Pickwin uses raw field files, either .dat, seg2, or segy files, and plots them in order to pick the first arrivals. The geometry must be set for the data, either during acquisition in the field using the seismograph or in the Pickwin program. The geometry is determined by setting the correct source and geophone locations; if not done correctly, the resulting velocity models can be incorrect. After the geometry has been set, a filter can be applied to the data, if necessary. By pressing CTRL-H in the Pickwin module, a 1000-Hz high-cut filter is applied to the field file; each subsequent use of CTRL-H multiplies the corner frequency by 0.8, so that a second use of CTRL-H applies an 800-Hz filter. For the low-cut filter, the first time CTRL-L is pressed, a 5-Hz low-cut filter, is applied to the field file, and each subsequent

use of CTRL-L increases the frequency by 1.5 Hz (Geometrics, 2009). In certain cases of excessive noise, bandpass filters were used. The most used bandpass filter settings for these data were low-cut 15 Hz, low-cut off 40 Hz, high-cut 45 Hz, and high-cut off 50 Hz.

The next step in the seismic-refraction processing was identifying and digitally picking the first break seismic arrivals. A first break is the first arrival of the direct or refracted seismic signal within the seismic trace (Veezhinathan and Wagner, 1990). Identifying and picking the correct signal are the first steps in creating an accurate velocity model. After the first breaks were picked, a file containing the pick files was loaded into the Plotrefra module. The pick files were converted to travel-time curves and were modified, corrected and checked for reciprocity. Because of errors in assigning first breaks, individual shotpoints often had to be modified in order to produce a more coherent velocity model.

The corrected travel times were quality tested by checking the reciprocal travel time. The principle of reciprocity states that the travel time measured between the source and the receiver should be the same in the reverse direction. Given that all subsurface conditions remain the same the travel times must be the same (OYO Corporation, 2009). Checking reciprocity is the primary means for evaluating data quality. Any data with a reciprocal error of more than 5 percent were evaluated with more scrutiny, because velocity models calculated from data with high reciprocal error are likely to be invalid. In most cases, this error can be attributed to poor first-break picking in the initial stages of the process. When the reciprocal error is too high to generate reliable velocity models, the

Plotrefra module offers an option to automatically correct reciprocal time. Often, a correction of individual shotpoints is needed following automatic correction.

In the near surface, absolute reciprocity cannot always be achieved, because of difficulty in picking the subtle first breaks; in these cases, it is essential to check and edit the arrival times. Subsequent to the travel-time curve reciprocity corrections, layer assignment is required. This process basically differentiates between the refractions generated from different layer boundaries. Based on the relationship between slope and velocity given in the equation below, the linear travel-time slopes will change as a function of the inverse of the velocities, thus defining a different layer.

Slope = 1/Velocity

Equation 2.1 Slope equation used in refraction analyses

In a near-surface investigation, the layer assignment is more difficult because of smaller variation in layer velocities. Similar velocities mean subtle breaks or changes in the travel-time slopes. Consequently, distinguishing layers is more problematic for generating accurate velocity models. The models produced by SeisImager software used the time-term inversion method. This technique inverts the first-arrivals by using linear-least squares and delay time analysis (OYO Corporation, 2009). The three major steps needed for creating a velocity model (Figure 2.2) are: first-break picking, velocity and layer assignment, and final inversion. How accurate the final inversion model is depends heavily on the accuracy of the first break picking.

2.2 Refraction Inversion Method

2.2.1 Time-Term Inversion

The time-term method utilizes a statistical linear least-squares approach to determine the layers from the given data in order to estimate the depth of given refractors. This method is comparatively faster than the reciprocal or tomographic approaches, because all that is needed is layer assignments for each of the first-break arrivals (Diabiase, 2004). The time-term inversion method assumes that all layers maintain a discrete constant velocity and a horizontal refractor interface (Diabiase, 2004).

2.3 Seismic Reflection

2.3.1 Seismic Reflection Acquisition

One common midpoint survey (CMP) was collected over a fault interpreted in Hunter's (2011) CUSSO 4 line in order to determine if the fault extended into the Quaternary stratigraphy; acquisition parameters for this survey are outlined in Table 2.4. In a CMP survey, the seismic source and receiver locations are moved along the direction of the inline spread so that subsurface boundaries are sampled at common discrete locations by multiple source-to-receiver travel paths. The survey was collected with a 48-channel Geometrics StrataVisor seismograph with two inline spreads of 24 Mark Products 30-Hz SH-wave geophones. A prior seismic walkaway sounding in the area indicated that an optimal recording window for the Quaternary section could be obtained by using a 2-m shot and geophone group spacing. The shear-wave energy source was a 1.8-kg sledgehammer for impact and an H-pile with a weight of approximately 70 to 80 kg, including the weight of the hammer swinger and the beam section. The H-pile flanges

were placed and struck perpendicular to the geophone spread and the direction of SH-wave propagation. The H-beam flanges were also placed in prepared slit trenches to resist movement and improve the energy couple with the ground. Seismograph polarity reversals and impacts of the sledgehammer on both sides of the energy source enhanced the SH-wave energy and decimated P-wave contamination. There was no offset of the energy source to the receiver array; thus the data were acquired by moving the energy source (H-beam and hammer) through the array. Six vertical stacks (i.e., multiple hammer hits per shot point station) were used for each shot point, three in the positive and three in the reversed polarity or negative directions. The data were saved to the seismograph's internal hard drive.

2.3.2 Seismic-Reflection Processing

The individual traces composing the optimal window within the 48-channel dataset were extracted and placed into a roll-along group file. Gather-files were constructed from the grouped field files, where each trace in the gather corresponds to a different source-to-receiver travel path that reflected from a common subsurface location (Mayne, 1962). Each gather trace was corrected to the zero-offset time and stacked (or added) with the other corrected traces in the gather. Figures 2.3 and 2.4 show an example of typical gather files at various stages of the processing sequences for both SH-and P-wave CMP surveys, respectively. The stages are: a) raw data, b) filtered, muted, and trace balanced, and c) moved out. The general procedure for the reprocessed Hunter (2011) lines as well as the SH-wave reflection survey, are shown in Table 2.5. The processing procedures for both surveys were the same with the exception of the filter parameters. The dominant frequency range analyzed on the Hunter (2011) profiles was 30-40 Hz.

Usable seismic reflection energy is usually confined by a bandpass width of approximately 10 to 70 Hz, with a dominant frequency around 30 Hz (Yilmaz, 1991). A bandpass filter of (15/25-70/80) was used during reprocessing in order to focus the amplitude spectrum over the dominant frequency range. Adaptive subtraction, deconvolution filtering, and noise attenuation were additional filtering algorithms used during reprocessing. Adaptive subtraction is used to suppress multiples and minimize noise (Ventosa et al., in press). Deconvolution was used twice during the processing. It was used the first time before the data were stacked, in order to suppress multiples and to increase resolution, and then it was applied the second time after the data had been stacked in order to further attenuate any multiples that were not sufficiently attenuated during the first deconvoluton process. After normal moveout, a threshold median noise attenuation filter was applied to reduce high amplitude noise. The additional filters improved the data quality and allowed for more detailed interpretations to be made in the near surface regions. Stack velocities and two-way travel times (TWTT) for all reinterpreted zones are in Tables 4.3 and 4.4, in addition to the Dix formula (Equation 4.1) used to calculate final interval velocities and thicknesses.

2.4 Seismic Resolution

2.4.1 Seismic Reflection and Refraction Resolution

Resolution is the ability to distinguish separate features. In reflection seismology, there are vertical and horizontal resolutions. Vertical resolution is the ability to distinguish reflections from the top and bottom of an interval (Geldart and Sheriff, 2004). In order to distinguish between two nearby reflective surfaces, they have to be $_{1/4}$

wavelength in thickness, which is called the $_{1/4}$ wavelength criterion where R is vertical resolution,

$$R= \lambda/4 = V/4f$$

Equation 2.2.

λ is wavelength, V is velocity, and f is frequency. Layers can still be detected (i.e., detectable limit) without distinguishing between the top and bottom, and are usually described by the $_{1/8}$ wavelength:

$$D= \lambda/8 =V/8f$$

Equation 2.3.

Vertical resolution decreases with distance traveled because of the attenuation of higher frequencies. A thickness less than $_{1/4}$ wavelength can be used to judge thickness, and for larger than $_{1/4}$ wavelength, wave shape can be used to judge thickness (Widess, 1973). Horizontal resolution describes how close two neighboring subsurface bodies can be to one another while still being recognizable as separate seismic events. This is a function of depth as well as frequency and velocity (Yilmaz, 1991). The area that produces the reflection is called the first Fresnel zone. Constructive interference of waves occurs in the first Fresnel zone, whereas subsequent energy effectively cancels out. The radius of the first Fresnel zone can be calculated by:

Equation 2.4. $$R_H = \frac{V}{2}\sqrt{\frac{t_0}{f}}$$

where V is velocity, t_o is two-way travel time, and f is frequency. Refraction resolution is constrained by array length and shot energy and, as a general approximation, the effective depth of the survey is usually $_{1/5}$ or $_{1/4}$ of the spread length (Abd-Aal and Mohamed, 2009).

Shear Wave Refraction Acquisition Parameters					
	CUSSO 1	**CUSSO 2**	**CUSSO 4**	**CUSSO 5**	**CUSSO 6**
Date of Survey	4/16/12	3/14/12	3/13/12	6/20/12	6/21/12
Source Type	4 lb. hammer	4 lb. hammer	4 lb. hammer	4 lb. hammer	4 lb. hammer
Source Deployment	5-10 times per station	5-10 times per station	5-10 times per station	5-10 times per station	5-10 times per station
Geophone Frequency	40 Hz SH-wave	40 Hz SH-wave	40 Hz SH-wave	40 Hz SH-wave	40 Hz SH-wave
Sample Rate	0.25 ms	0.25 ms	0.25 ms	0.25 ms	0.25 ms
Acquisition Filters	Low: 15 Hz High: Off Notch: 60 Hz	Low: 15 Hz High: Off Notch: 60 Hz	Low: 15 Hz High: Off Notch: Off	Low: 15 Hz High: Off Notch: 60 Hz	Low: 15 Hz High: Off Notch: 60 Hz
Source Stations	56	70	56	21	21
Geophone Interval	4 m	4 m	4 m	4 m	4 m
Geophone Group Channels	2 X 24	2 X 24	2 X 24	2 X 24	2 X 24
Offset	±48 m	±48 m	±48 m	±48 m	±48 m
Record Length	2,000 ms	2,000 ms	2,000 ms	1,024 ms	1,024 ms
Site Surveyed	Sassafras Church Road	Running Slough Road	State Highway 971	State Highway 94	Cotton Gin Road
Total Profile Length	956 m	1050 m	860 m	380 m	380 m

Table 2.1. Acquisition parameters for 4-m CUSSO full refraction lines.

Shear Wave Refraction Sounding Tests Acquisition Parameters				
	CUSSO 2	**CUSSO 4**	**CUSSO 3**	**CUSSO 4**
Date of Survey	07/14/11	07/15/11	12/30/11	6/20/12
Source Type	4 lb. hammer	4 lb. hammer	4 lb. hammer	4 lb. hammer
Stack per Station	6-8 times	8-14 times	14 times	10 times
Geophone Frequency	30 Hz SH-wave	30 Hz SH-wave	30 Hz SH-wave	30 Hz SH-wave
Sample Rate	0.25 ms	0.25 ms	0.25 ms	0.50 ms
Acquisition Filters	Low: 15 Hz High: Off Notch: 60 Hz	Low: 15 Hz High: Off Notch: 60 Hz	Low: 15 Hz High: Off Notch: Off	Low: 15 Hz High: Off Notch: Off
Source Stations	7	7	5	4
Geophone Interval	2 m	2 m	4 m	4 m
Geophone Group Channels	2 X 24	2 X 24	2 X 24	2 X 24
Offset	± 2 and 48 m	± 2, 48, and 90 m	None	None
Record Length	1,024 ms	1,024 ms	1,024 ms	1,024 ms
Site Surveyed	Running Slough Road	Highway 94	Chesshire Lane	Highway 94
Total Profile Length	96 m	96 m	192 m	192 m

Table 2.2. Acquisition parameters for refraction sounding tests.

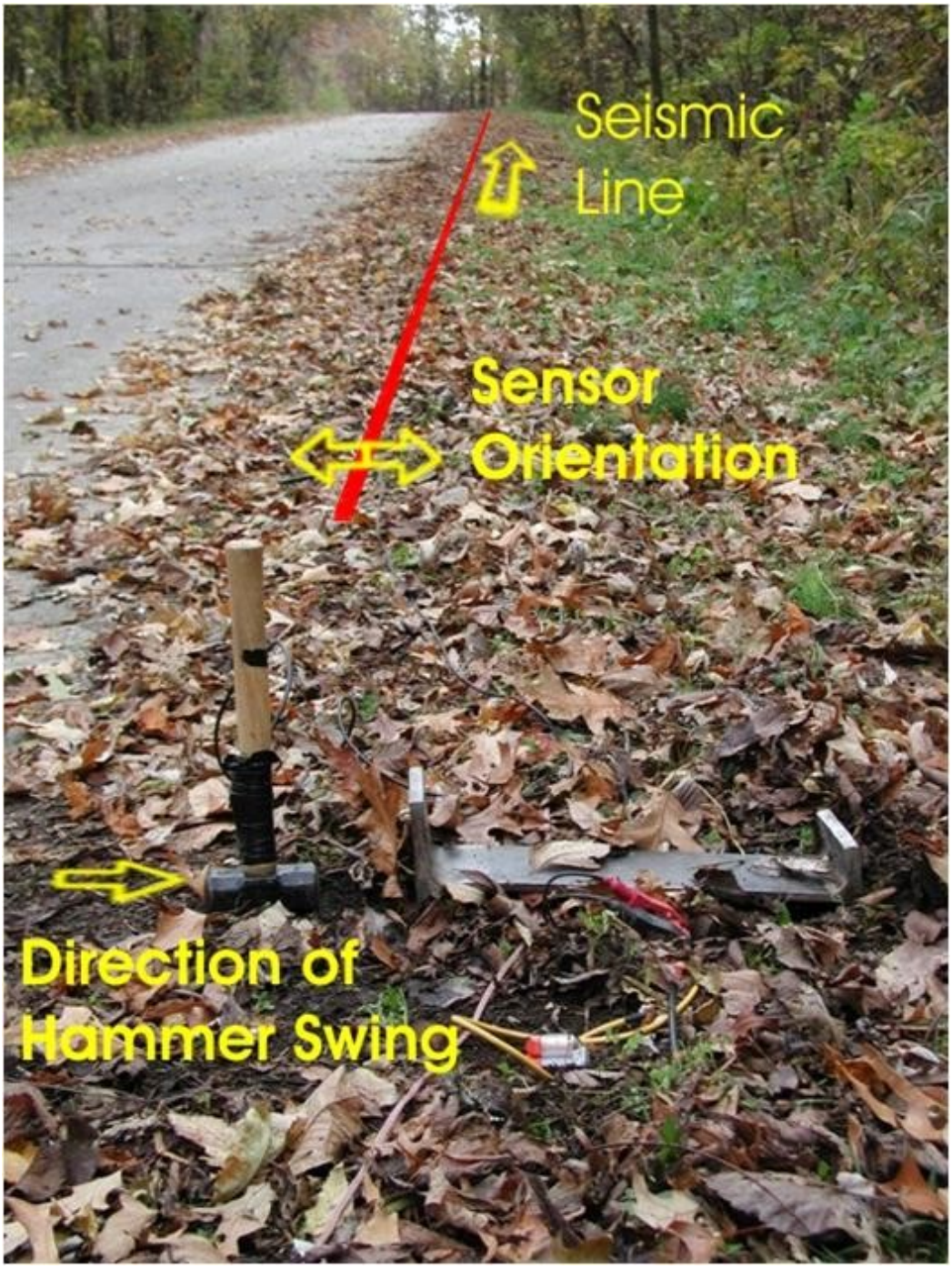

Figure 2.1. The typical set-up for shear-wave refraction acquisition. The H-beam lies flat and is coupled to the ground as the hammer source strikes both sides of the beam (Rutledge, 2004).

	Offset (-48 m)	Geophone 1	Geophone 12	Geophone 24	Geophone 36	Geophone 48	Offset (+48 m)
First 48 m	-48	0	48	96	144	192	240
First Roll Along (24 m)	48	96	144	192	240	288	336
Second Roll Along (24 m)	144	192	240	288	336	384	432
Third Roll Along (24 m)	240	288	336	384	432	480	528
Fourth Roll Along (24 m)	336	384	432	480	528	576	624
Fifth Roll Along (24 m)	432	480	528	576	624	672	720
Sixth Roll Along (24 m)	528	576	624	672	720	768	816
Seventh Roll Along (24 m)	624	672	720	768	816	864	912
Eighth Roll Along (24 m)	720	768	816	864	912	960	1008
Ninth Roll Along (24 m)	816	864	912	960	1008	1056	1104

Table 2.3. Geometry parameters for a 48-channel survey with four additional 24 m roll-along surveys.

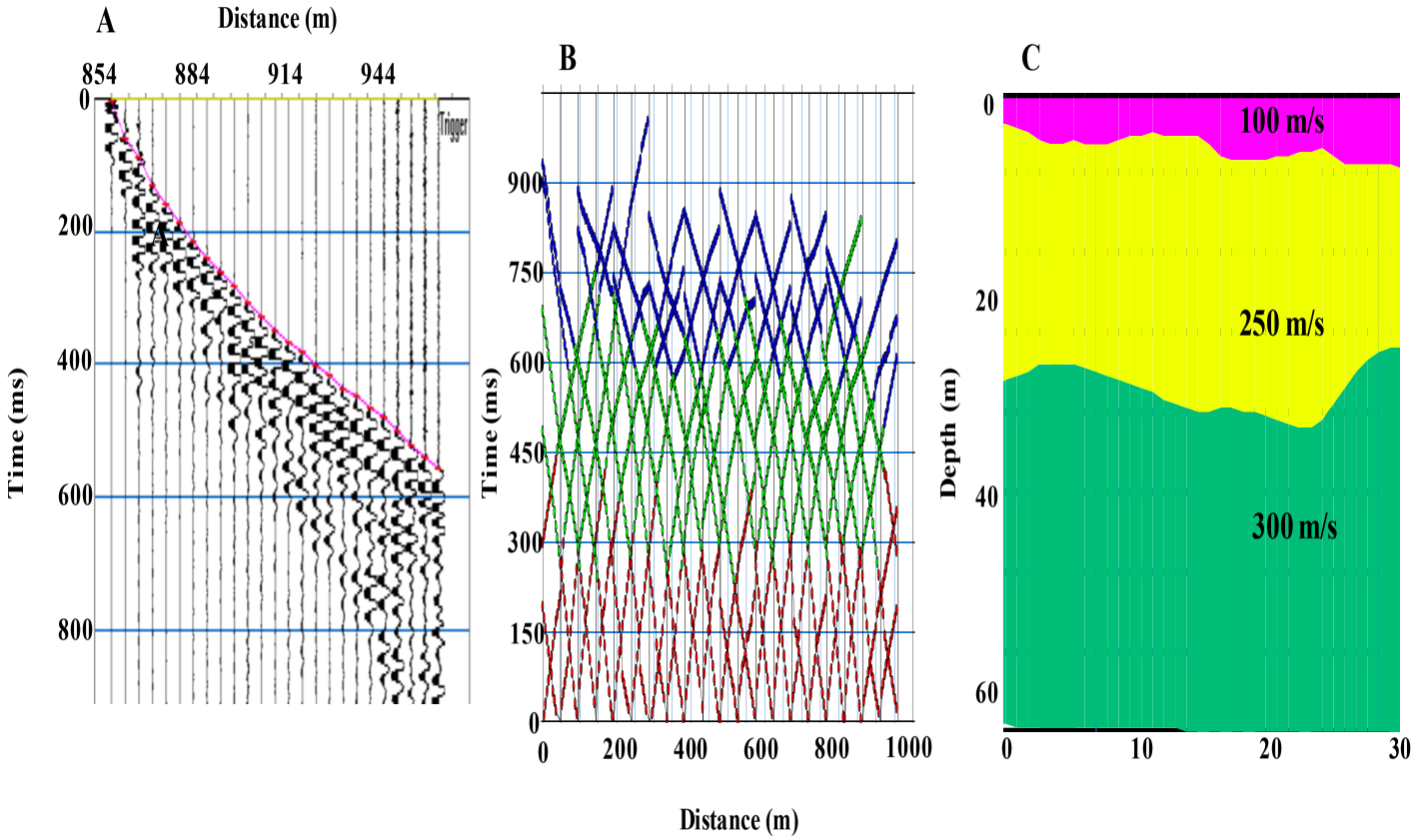

Figure 2.2. Three steps in the refraction process (A - C). (A) The initial fields file with first break interpretations. (B) The first-break interpretations or travel time curves for all field files at CUSSO 1; once these files have been plotted, layer interpretations can be determined. (C) A time-term inversion velocity model, the final step in the refraction method.

Shear Wave Reflection Acquisition Parameters	
	CUSSO 6
Date of Survey	6/21/12
Source Type	4 lb. hammer
Source Deployment	3-4 times per station
Geophone Frequency	40 Hz SH-wave
Sample Rate	.50 ms
Acquisition Filters	Low: 15 Hz High: Off Notch: Off
Source Stations	215
Geophone Interval	2 m
Geophone Group Channels	2 X 24
Source Offset	None
Record Length	2,000 ms
Fold	12
Site Surveyed	State Highway 971
Total Profile Length	424 m

Table 2.4. The acquisition properties for a shear wave reflection line done over the CUSSO 4 line.

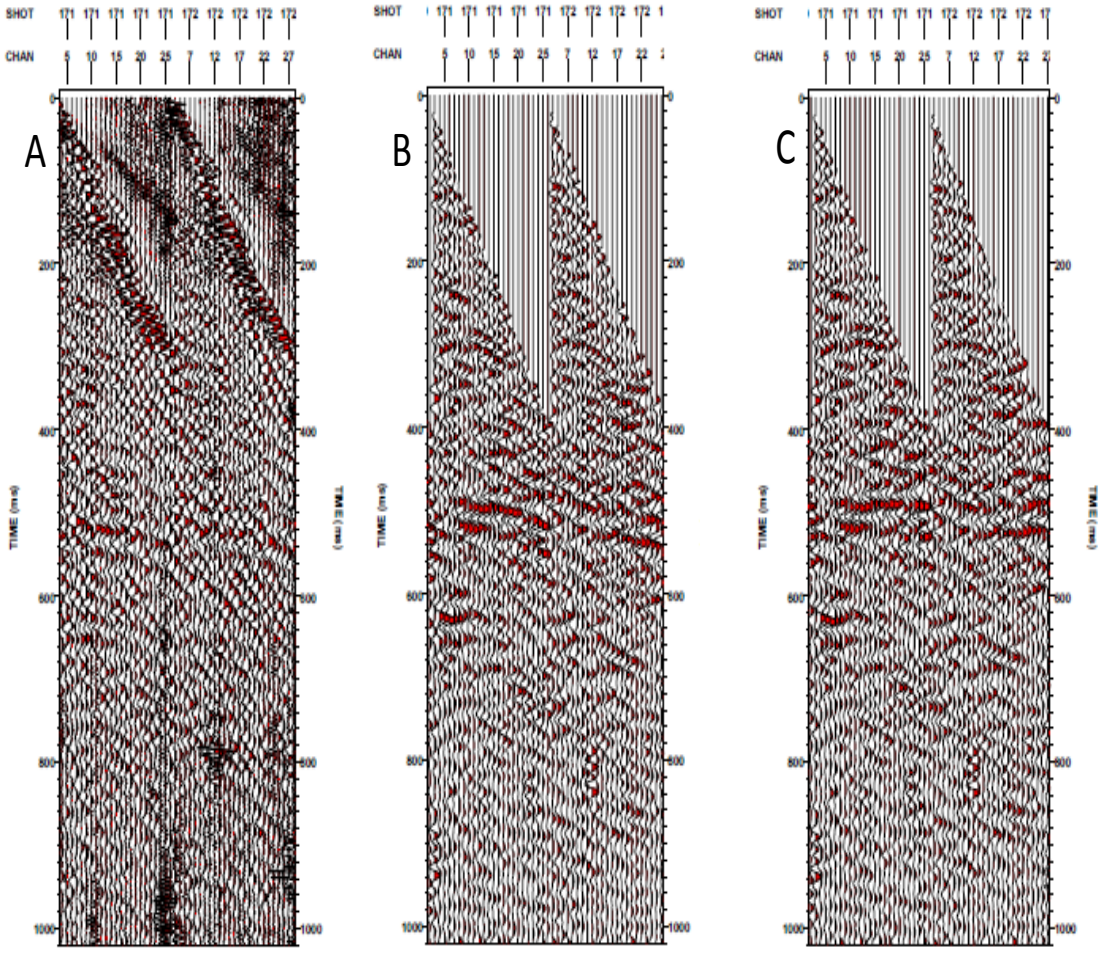

Figure 2.3. SH-Wave processing images. (A) Field files after geometry and automatic gain control have been applied. (B) The same lines, after a filter has been applied and then deconvolution performed. (C) The lines, after velocity analysis and normal moveout have been applied.

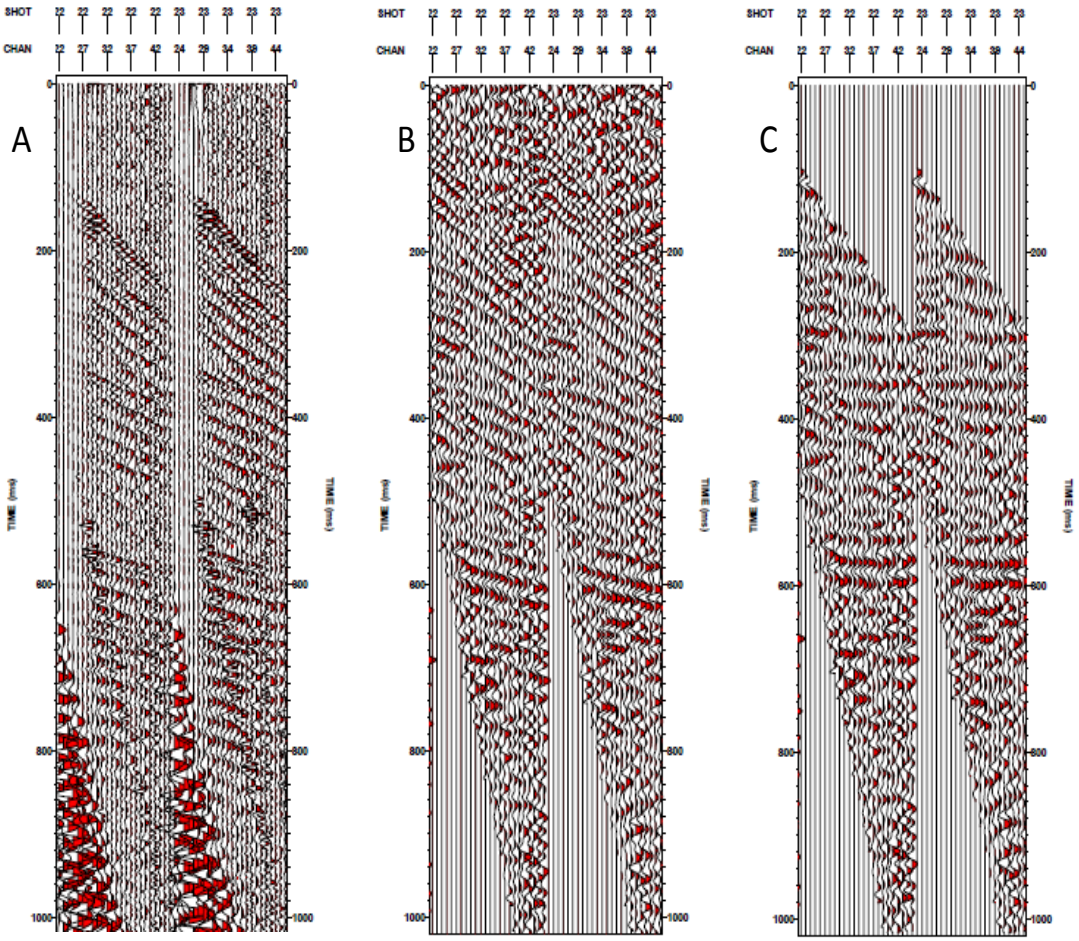

Figure 2.4. P-Wave processing images. (A) Field files after geometry and automatic gain control have been applied. (B) The same lines, after a filter has been applied and then deconvolution performed. (C) The lines, after velocity analysis and normal moveout have been applied.

General Processing Procedure
1. Reformat from SEGY to internal Vista format
2. Input array geometry
3. Time-variant scaling
4. Data scaling
5. Ormsby band-pass filter
6. Data scaling
7. Mute traces
8. FK filter
9. Adaptive subtraction
10. Deconvolution (spiking)
11. Normal move-out correction
12. Threshold median noise attenuation
13. Common midpoint stack
14. Deconvolution (spiking) plus pre-whiting

Table 2.5. The general P-and SH-wave reflection survey reprocessing procedures in Vista 11 software.

	Stack Velocity (~RMS)	TWTT
Zone 1	**1482 m/s**	**.212 s**
Zone 2	**1583 m/s**	**.184 s**
Zone 3	**1688 m/s**	**.350 s**
Zone 4	**1882 m/s**	**.549 s**
Zone 5	**2022 m/s**	**.630 s**

Table 4.3. Stack velocities and two-way travel times (TWTT) from major seismic reflection horizons interpreted on P-wave reflection lines (CUSSO 1-4).

	Stack Velocity (~RMS Velocity)	TWTT
Zone 1	**184 m/s**	**.115 s**
Zone 2	**294 m/s**	**.322 s**
Zone 3	**395 m/s**	**.529 s**

Table 4.4. Stack velocities, two-way travel time (TWTT) from major seismic reflection horizons interpreted on SH-wave reflection line (CUSSO 4).

Dix formula:

$$V_{int} = [(t2*V_{rms}2^2-t1*V_{rms}1^2)/(t2-t1)]^{1/2}$$

Where V_{int} = interval velocity

$t1$ = travel time of the first reflector

$t2$ = travel time of the second reflector

$V_{rms}1$ = root-mean-square velocity of the first reflector

$V_{rms}2$ = root-mean-square velocity of the second reflector

$$H_n = V_{int}(t_o2-t_o1)/2$$

Where H_n = Height

V_{int} = interval velocity

t_o1 = travel time of the first reflector

t_o2 = travel time of the second reflector

Equation 4.1. Dix Formula used to calculate interval velocities, heights, and depths for reflection data.

CHAPTER THREE: REFRACTION MODELS

3.1 Final CUSSO Refraction Lines

The 4 m CUSSO full-survey refraction lines provide relevant information about the Quaternary and upper Eocene seismic boundaries. The five 4 m surveys consisted of 21 to 70 source locations with two to nine roll-alongs. The energy source locations were at geophones 1, 12, 24, 36, and 48. Additional shot-points were located 48 m off the ends of the geophone array. Lines 1, 2, and 4 are 956, 1050, and 860 m in length, respectively. Both lines 5 and 6 are 380 m in length.

3.1.1 Four-Meter CUSSO 1 Refraction Line

The velocity model for the CUSSO 1 line (Figure 3.1-A) contains three distinct velocity layers. The first layer has an average thickness of 16 m and a velocity of 160 m/s. The second layer has an average thickness of 25 m and a velocity of 275 m/s. Both the first and second layers correlate to Quaternary sediments. The third layer has a velocity of 406 m/s and corresponds to upper Eocene sediments. The velocity difference between the two layers that corresponds to Quaternary sediments may be caused by the transition from coarse to fine sands in the Quaternary or the level of compaction of the sediments.

3.1.2 Four-Meter CUSSO 2 Refraction Line

The model for the CUSSO 2 line (Figure 3.1-B) shows approximatley 35 to 45 m of Quaternary sediments before the top of the Eocene. The first layer is, on average, 15 m thick and has a velocity of 131 m/s. The first layer interpreted at the CUSSO 2 location is similar to the first layer at CUSSO 1. The second interpreted velocity layer at CUSSO 2

has an average thickness of 17 m and a velocity of 285 m/s. This is most likely the same velocity layer that was interpreted at CUSSO 1; although the thickness at this site is nearly 10 m less than at CUSSO 1. The third layer has a velocity of 402 m/s and correlates to Eocene sediments. Although slightly southwest of the CUSSO 1 line, all three layers in both models remain consistent.

3.1.3 Four Meter CUSSO Four Refraction Line

The CUSSO 4 (Figure 3.1-C) model has an average of 45 m of Quaternary sediments before the top of Eocene sediments. The first layer has an average thickness of 17 m and velocity a of 149 m/s. The velocity of this layer is between the values calculated for the CUSSO 1 and 2 lines. The second layer has an average thickness of 27 m and a velocity of 243 m/s. The third layer has a velocity of 349 m/s. This velocity is slightly lower than expected for a thrid layer, when compared to other models. This third layer correlates in depth to upper Eocene sediments. All three last layers velocites for this east-west line are slightly lower than expected based on depth and may be caused by a subtle lithologic change.

3.1.4 Four-Meter CUSSO 5 Refraction Line

The model for the CUSSO 5 (Figure 3.1-D) line represents the survey that was closest to the borehole. The first layer has an average thickness of 12 m of Quaternary sediments and a velocity of 181 m/s, and it is the fastest first layer in the study. The second layer has an average thickness of 18 m and a velocity of 210 m/s. The third layer has an average thickness of 21 m and a velocity of 294 m/s. The second and third layers correlated to Quaternary sediments and represent a subtle transition between Quaternary and upper Eocene sediments.

3.1.5 Four-Meter CUSSO 6 Refraction Line

The model for the CUSSO 6 (Figure 3.1-E) line has a first layer with an average thickness of 13 m and a velocity of 160 m/s. The velocity for this layer is consistent with the other 4 m CUSSO lines at this average depth. The second unit ranges in thickness from 18 to 34 m, and the velocity associated with this layer is 210 m/s and corresponds with the second layer on the CUSSO 5 model. The third layer has a velocity of 304 m/s and, similar to layers 1 and 2, corresponds to Quaternary sediments.

3.1.6 Four Meter Full Refraction Survey Results

All five of the full survey CUSSO lines discussed above contained a first layer that was similar in velocity and depth. The velocity ranges from 131 m/s up to 181 m/s and depth averages 15m. The second layer has a velocity between 210 m/s and 310 m/s. It is probable that based on common depths and velocities, layers 2 and 3 from CUSSO models 5 and 6 represent a single layer. The third layer has a velocity range between 349 and 406 m/s, and was only interpreted on models 1, 2, and 4. Figure 3.2 shows the combined layer interpretations for the final CUSSO refraction lines.

3.2 Sounding Tests

Both the 2-and 4-m sounding tests provided preliminary information regarding an optimal array size to sample the Quaternary velocity structures in the production surveys. The 2- and 4-m meter soundings were derived from four to seven source locations with one to three roll-alongs. The energy source locations were at geophones 1, 12, 24, 36, and 48. Additional shotpoints were located at 2, 48, and 98 m off the ends of the geophone array. The 2-m sounding tests were conducted prior to the 4-m tests between July 11 and 15, 2011, and consisted of two test surveys: along the CUSSO 2 line and along the

CUSSO 4 line. The 2-m results used 48 30-Hz SH-wave geophones totaling 92 m. Two 4-m soundings were collected the at CUSSO 3 and CUSSO 4 lines, totaling 190 m each.

3.2.1 Two-Meter CUSSO 2 Sounding

The upper unit at the CUSSO 2 site (Figure 3.3-A) is 4 to 8 m thick and the velocity associated with this interval is 110 m/s. The second unit has a velocity of 213 m/s and is 4 to 16 m thick. The third unit has a velocity of 277 m/s. All three units correlate with Quaternary sediments. The velocity is not considerably faster in the second and third intervals and may be the result of a slight lithologic difference between the two intervals.

3.2.2 Two-Meter CUSSO 4 Sounding

Along the CUSSO 4 line, (Figure 3.3-B) two refraction velocity layers were interpreted. The first has a velocity of 140 m/s and an average thickness of 9 m. This layer correlates in depth to the first interval layer in the CUSSO 2 test. The velocity difference between the first layers at CUSSO 4 and CUSSO 2 is 30 m/s, but the layer at this site has a larger average thickness and may be extending into a faster velocity layer at the base. The second layer in this model had a velocity of 238 m/s. This layer correlates to the second layer at CUSSO 2. Both layers in this sounding test correlated to Quaternary sediments.

3.2.3 Two-Meter CUSSO Sounding Results

The 2-m velocity models each contained two layers that were found at both sites and then a third zone that was only found at one site. The first major refraction boundary in both models had an average thickness of about 9 m and velocity ranging from 110 to

140 m/s. The second interval has an average thickness ranging from 9-12 m and velocities from 213 to 238 m/s. The third unit found at CUSSO 2 may be very similar to that in layer 2. With a velocity of 277 m/s, this layer is only slightly faster and correlates to Quaternary sediments, as in the other two layers.

3.2.4 Four-Meter CUSSO 3 Sounding

The uppermost layer interpreted at the CUSSO 3 (Figure 3.3-C) sounding ranged in depth between 3 and 10 m with an average depth of 6 m. The velocity in this unit is 158 m/s, which is slightly higher than the velocities for the 2-m spacing tests at the same location. The second layer has a velocity of 208 m/s and a depth ranging between 11 and 27 m. The third layer in the model has a velocity of 237 m/s. The difference in seismic velocity between the last two units is very subtle and may be attributed to the amount of coarse material in the third unit or differences in the degree of compaction. All layers correlate to Quaternary sediments.

3.2.5 Four-Meter CUSSO 4 Sounding

The upper layer at CUSSO 4 (Figure 3.3-D) has an average thickness of 8 m and velocity of 137 m/s. The second layer has a velocity of 215 m/s and an average thickness of 19 m. The third layer has a velocity of 277 m/s to the third unit at the CUSSO 2. Depths and velocities calculated within this layer are comparable to other soundings and correspond to Quaternary sediments.

3.2.6 Four-Meter CUSSO Sounding Results

The results of both sounding tests yielded four distinct near-surface layers. The first layer, found on all four tests, ranges from 5 to 9 m in thickness and 110 to 158 m/s in

velocity. This layer corresponds to Quaternary sediments, according to the well-log descriptions. The second layer was interpreted at 4 m at both CUSSO 3 and CUSSO 4 and at 2 m at CUSSO 2. Thickness ranged from 12 to 19 m and velocity between 209 and 213 m/s, and correlates to Quaternary sediments. The third velocity layer was interpreted at 4 m at CUSSO 3 and 2 m at CUSSO 4 and was very similar in thickness and velocity. At CUSSO 3, the thickness and velocity are 11 m and 238 m/s respectively, and at CUSSO 4 thickness is 10 m and velocity is 239 m/s. The last velocity layer was interpreted at 4 m from CUSSO 4 data and had a slightly higher velocity of 275 m/s, when compared to the other layers.

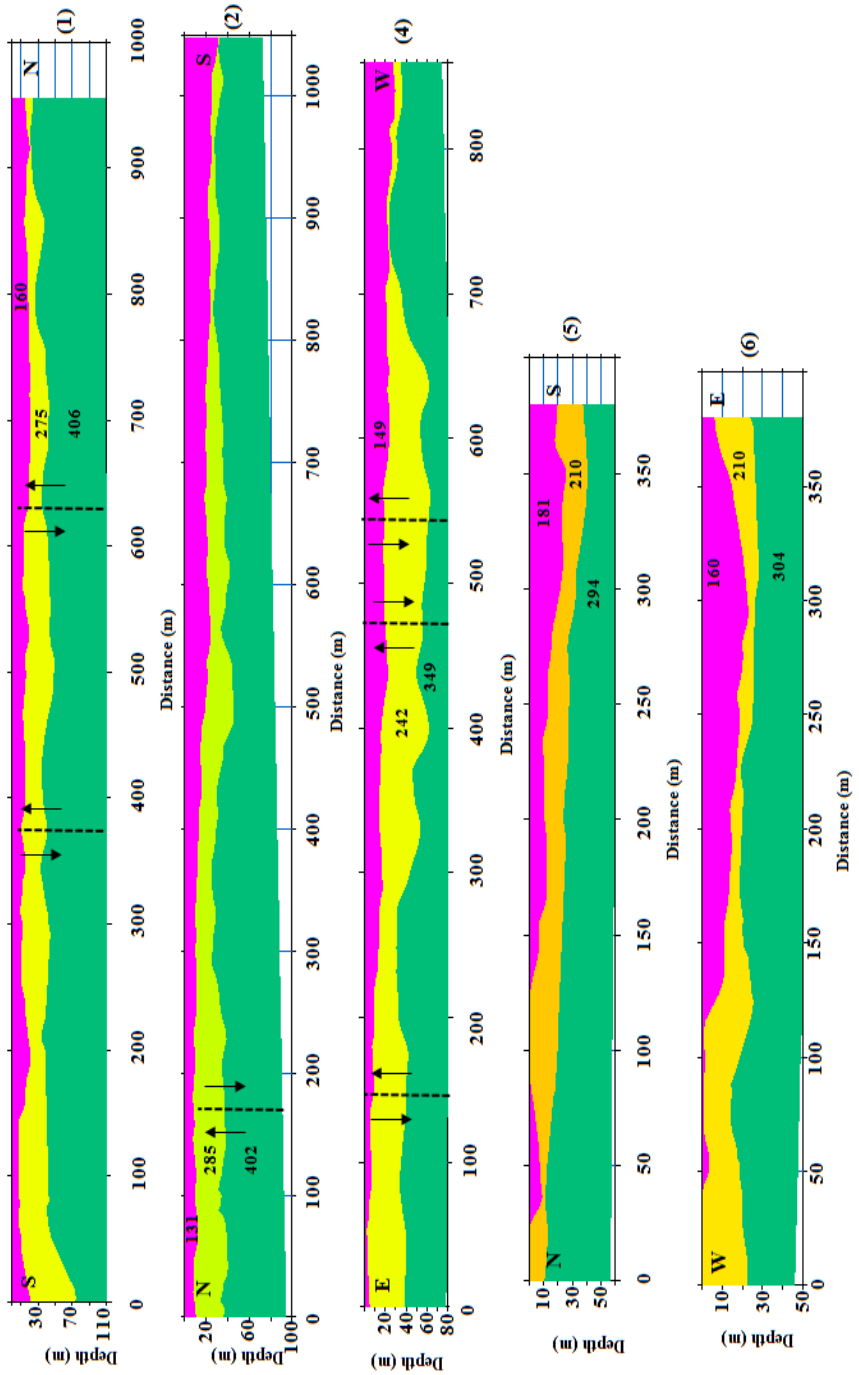

Figure 3.1. Four-meter final refraction surveys. A-E correspond to CUSSO lines 1, 2, 4, 5, and 6, respectively. Black lines are previously interpreted faults from P-wave reflection data. These faults were interpreted to offset horizons in the Paleozoic through Paleocene.

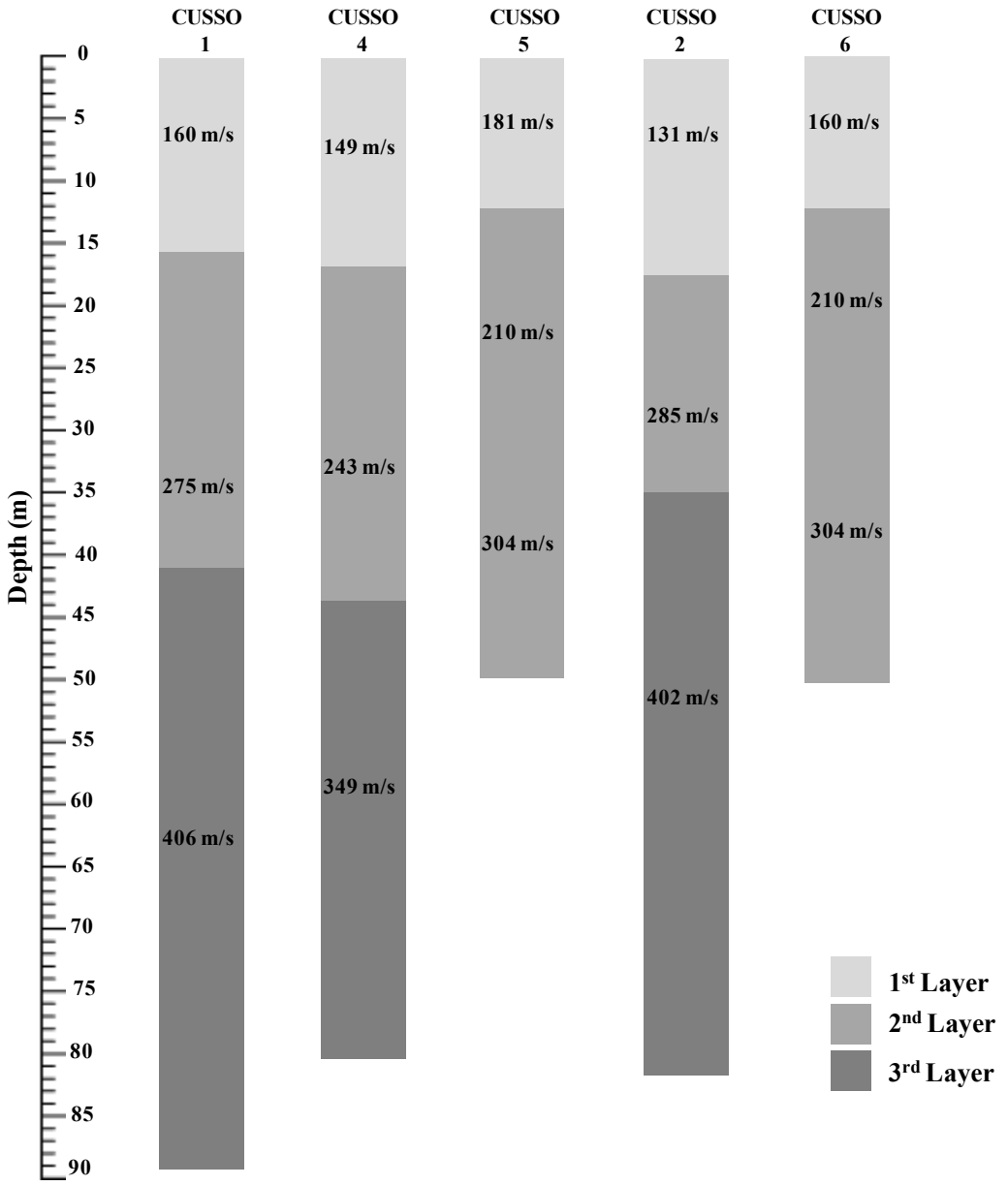

Figure 3.2. Refraction results from full four meter lines. Three major velocity zones are represented above and correlate to Quaternary and upper Eocene sediments.

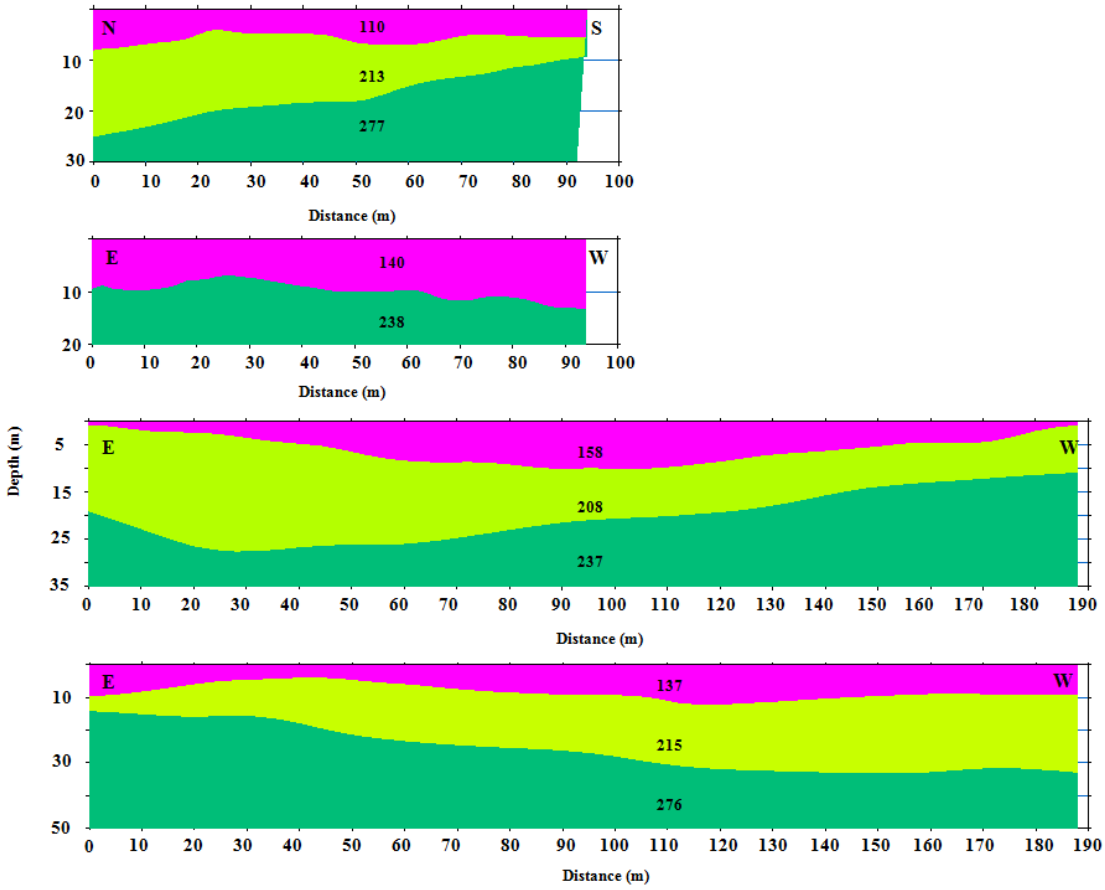

Figure 3.3. Two- and Four-meter CUSSO soundings. (A) and (B) are both 2 m. Figure A is along CUSSO 2, and (B) is along CUSSO 4. (C) and (D) are both 4 m spacing. (C) is along CUSSO 3, and (D) is along CUSSO 4.

CHAPTER FOUR: SEISMIC REFLECTION

4.1 CUSSO Reflection Analysis

Reflection lines were reprocessed using more robust signal-processing algorithms (i.e., VISTA11 software) that have recently become available to the University of Kentucky. The reprocessed data were reinterpreted in order to characterize any significant impedance boundaries above the Cretaceous horizon that may have been obscured in previous studies. After reprocessing, the data were reinterpreted to have revealed five continuous reflectors apparent on all four lines. Faults that appeared to extend into Eocene and Quaternary boundaries were also reinterpreted.

The tops of zones 1-5 correlated to the Quaternary/Eocene, Eocene Claiborne, Eocene Wilcox, Cretaceous McNairy, and Paleozoic bedrock, respectively. The tops of zones 1 and 2 along the south-north CUSSO 1 line (Figure 4.1) are at approximately 130 ms and 160 ms TWTT. Both reflectors appear to become less coherent between traces 125-170. The top of the third zone is located approximately 380 ms and is coherent throughout. The tops of zones four and five are located at 540 and 640 ms, respectively and are similar to Hunter's (2011) findings; they were the two most coherent reflectors for all of the CUSSO lines. The top of zone 1 along the north-south-oriented CUSSO 2 line is found at approximately 115 ms and truncates around trace 100 (Figure 4.2). The tops of zones 2 and 3 are at approximately 160 and 380 ms, respectively, and unlike the case with the CUSSO 1 line zones 2 and 3 are more coherent throughout CUSSO 2. The top of the fourth zone is located at approximately 540 ms, and the top of the fifth zone is at 610 ms. The top of zone 1 along the east-west CUSSO 3 (Figure 4.3) line is at approximately 130 ms and is coherent throughout the line. The top of zone 2 is around

160 ms and the reflector disappears near the western edge of the line, near an interpreted fault location. The top of zone 3 is approximately 350 ms, and 540 ms is the top of zone four. The top of zone 5 is approximately 610 ms and is coherent throughout the line. The top of zone 1 along the east-west-oriented CUSSO 4 line is around 120 ms, and the top of zone 2 is approximately 140 ms. Both reflectors truncate near trace 125. The tops of zones 3 and 4 are near 300 and 520 ms, respectively. The top of the Paleozoic bedrock along CUSSO 4 (Figure 4.4) line is interpreted to be around 620 ms. All of the two-way travel times associated with the reinterpreted horizons are listed in Table 4.1.

4.2 Fault Zone Interpretations

Abrupt termination of continuous reflectors and changes in the dip of the reflector were also considered. At least three high-angle faults were imaged and extend through the Paleozoic and Cretaceous sediments. In some instances there does appear to be offset in the Eocene sediments. Further research is needed to conclude if these faults continue into near surface Quaternary sediments. Interpreted structural features and faults in this study are in agreement with interpretations made in the Hunter (2011) study.

Faults one and two, along CUSSO, are located between traces 140 and 110 and 100 and 68, respectively. Vertical offset on the south sides of the faults appear to be shifted up 60 ms and 30 ms for the Paleozoic and Cretaceous reflectors, accordingly. Fault three, interpreted on CUSSO 2, offsets the lower impedance boundaries by nearly 70 ms and is the easternmost of the three faults. Faults one and two interpreted along CUSSO 3 show offset of approximately 25 ms and offset Paleozoic and Cretaceous horizons. Faults interpreted at CUSSO 4 appear to offset bedrock and Cretaceous reflectors by approximately 35 ms and 25 ms, respectively. Fault one and two were

interpreted to be between trace numbers 80-89 and 37-48. An additional fault was interpreted between trace numbers 110-120 and may be associated with fault one and it appears that between traces 80-120 there is a fault bound deformation zone. To better image this zone a supplementary survey was collected.

4.3 CUSSO 4 Fault Interpretation

A 12-fold 20-m SH-wave common midpoint survey was shot over traces 80-120 along the end of the CUSSO 4 line. This was one of eight prominent structural features found by Hunter (2011) and was judged to be a likely candidate for projecting a near-surface expression. Figure 4.9 shows the detailed 4-m-spacing SH-wave line. The shallow reflection line shows three prominent impedance boundaries with TWTT of 115, 322, and 529 ms. The offset associated with the lower boundary is approximately 18ms, with a coherent reflector for most of the survey except between traces 0 and 100. The middle reflector located around 322 ms is coherent from traces 100-330 and has a reflector offset of approximately 15ms. The final continuous reflector in the survey has a layer boundary that had an average TWTT of approximately 155 ms. This reflector was relatively coherent throughout the survey except for traces 0-70. The offset associated with this reflector is around 20 ms.

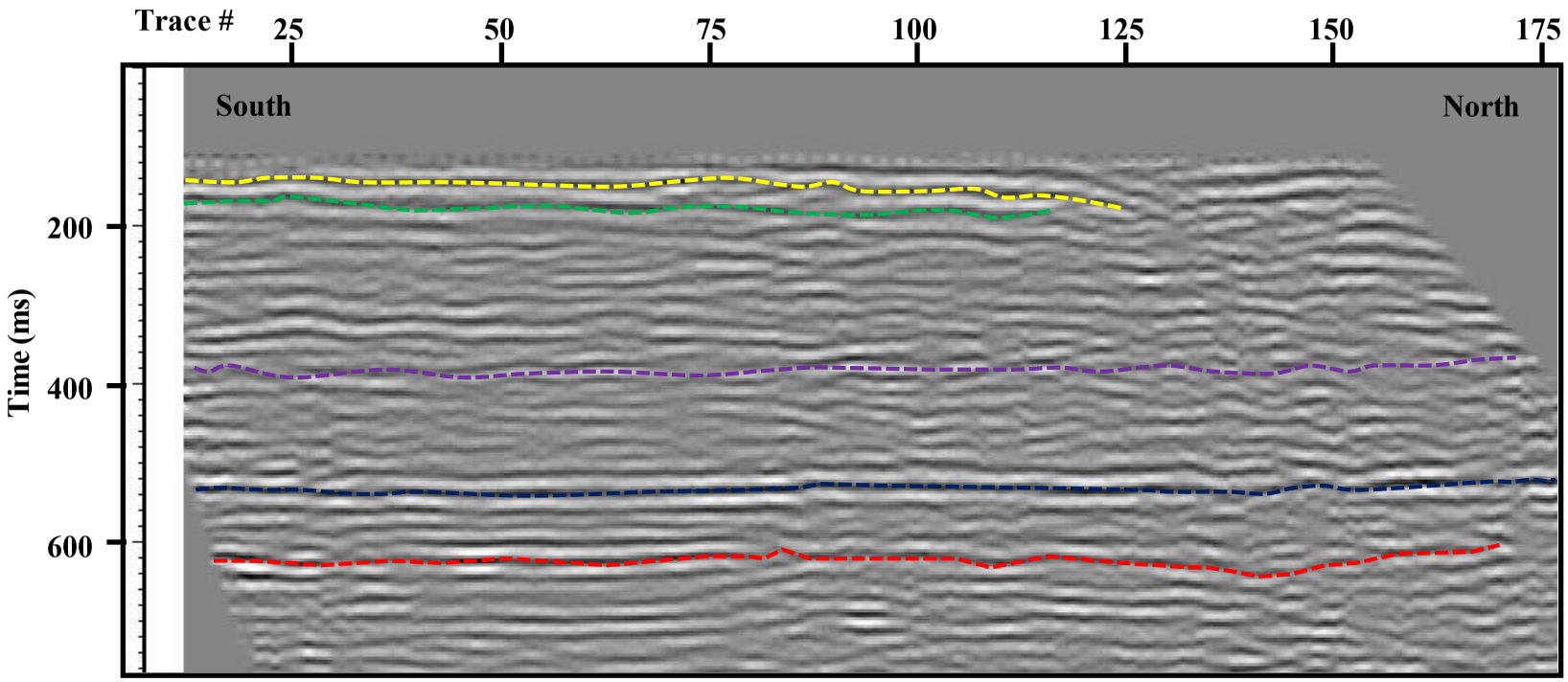

Figure 4.1. The reinterpretation of the CUSSO 1 line. The lower three coherent boundaries correlate with the Paleozoic bedrock (red), Cretaceous McNairy (blue), and the top of the Eocene Wilcox/Paleocene Porter's Creek Formations (purple). The tops of the upper two boundaries are less coherent than the lower three and represent the Eocene Claiborne (green) and the Eocene Jackson (yellow).

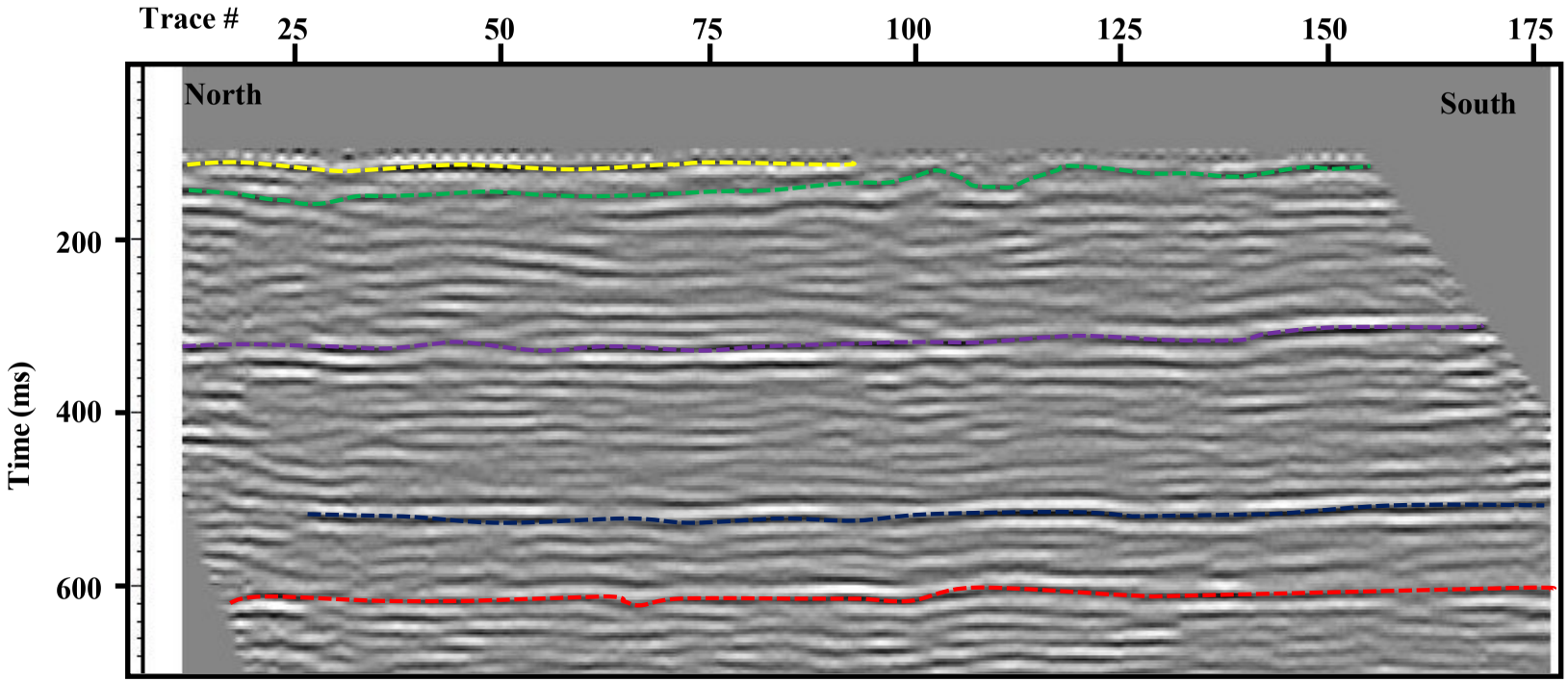

Figure 4.2. Reinterpretation of the CUSSO 2 line. The lower three coherent boundaries correlate with the Paleozoic bedrock (red), Cretaceous McNairy (blue), and the top of the Eocene Wilcox/Paleocene Porter's Creek Formations (purple). The Eocene Claiborne (green) is fairly coherent along this line. The Eocene Jackson (yellow) is coherent along much of the line and becomes less coherent beyond trace 100.

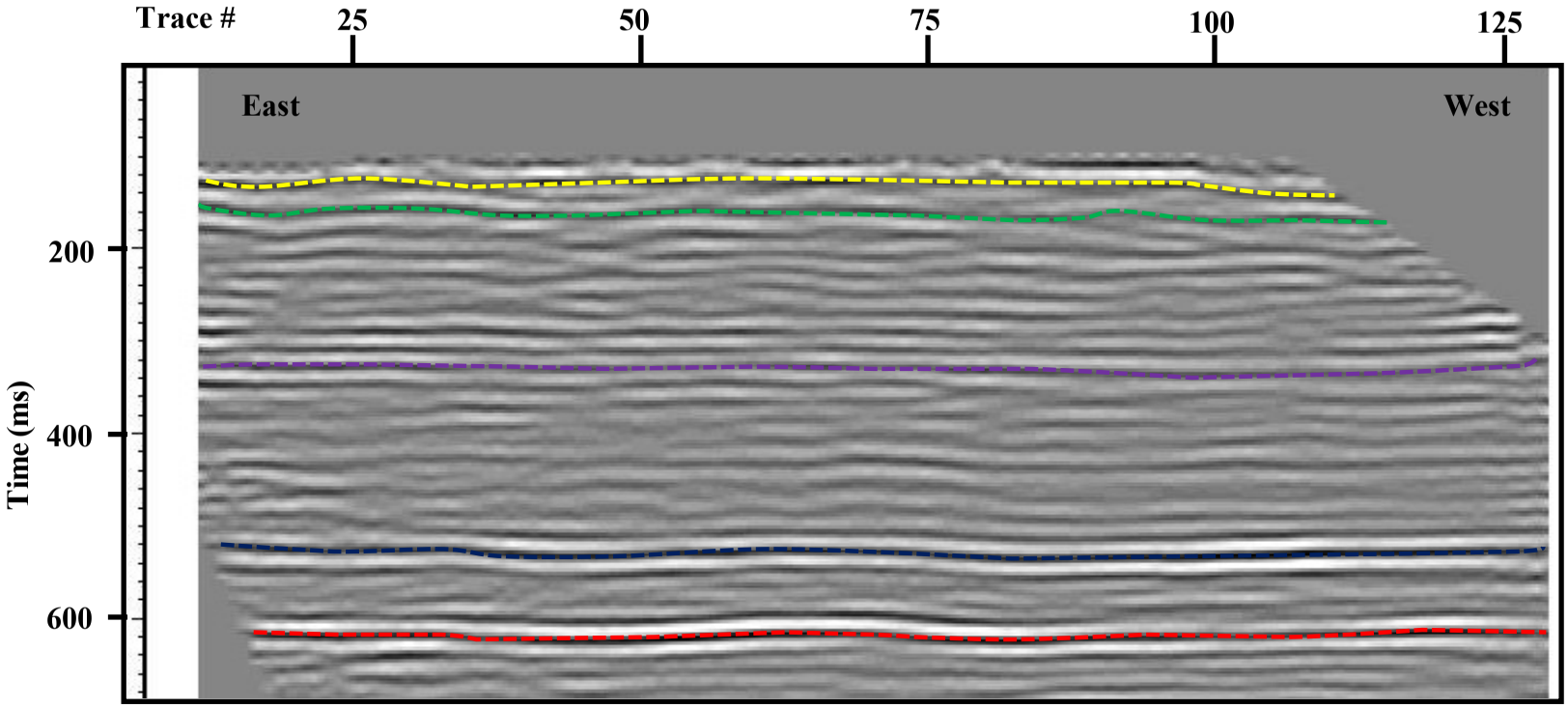

Figure 4.3. Reinterpretation of the CUSSO 3 line. The lower three coherent boundaries correlate with the Paleozoic bedrock (red), Cretaceous McNairy (blue), and the top of the Eocene Wilcox/Paleocene Porter's Creek Formations (purple). The tops of the upper two boundaries are coherent along the full survey represent the Eocene Claiborne (green) and the Eocene Jackson (yellow).

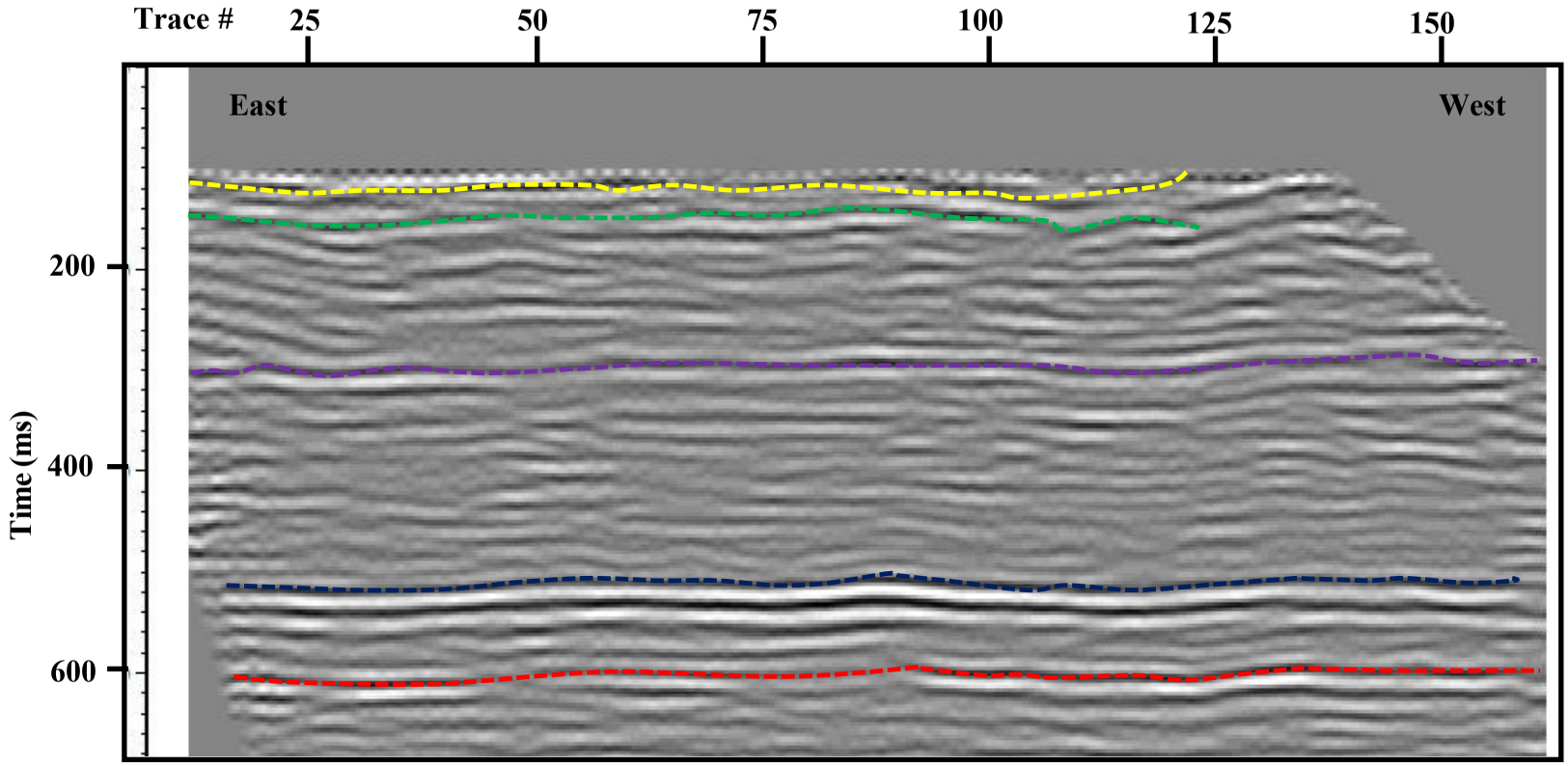

Figure 4.4. Reinterpretation of the CUSSO 4 line. The lower three coherent boundaries correlate with the Paleozoic bedrock (red), Cretaceous McNairy (blue), and the top of the Eocene Wilcox/Paleocene Porter's Creek Formations (purple). The tops of the upper two boundaries are less coherent than those ofthe lower three and represent the Eocene Claiborne (green) and the Eocene Jackson (yellow).

Site	Zone 5	Zone 4	Zone 3	Zone 2	Zone 1
CUSSO 1	640 ms	540 ms	380 ms	160 ms	130 ms
CUSSO 2	610 ms	540 ms	340 ms	160 ms	115 ms
CUSSO 3	610 ms	540 ms	350 ms	160 ms	130 ms
CUSSO 4	620 ms	520 ms	300 ms	140 ms	120 ms

Table 4.1. Two-way travel times from major seismic reflection horizons on reinterpreted CUSSO lines (1-4).

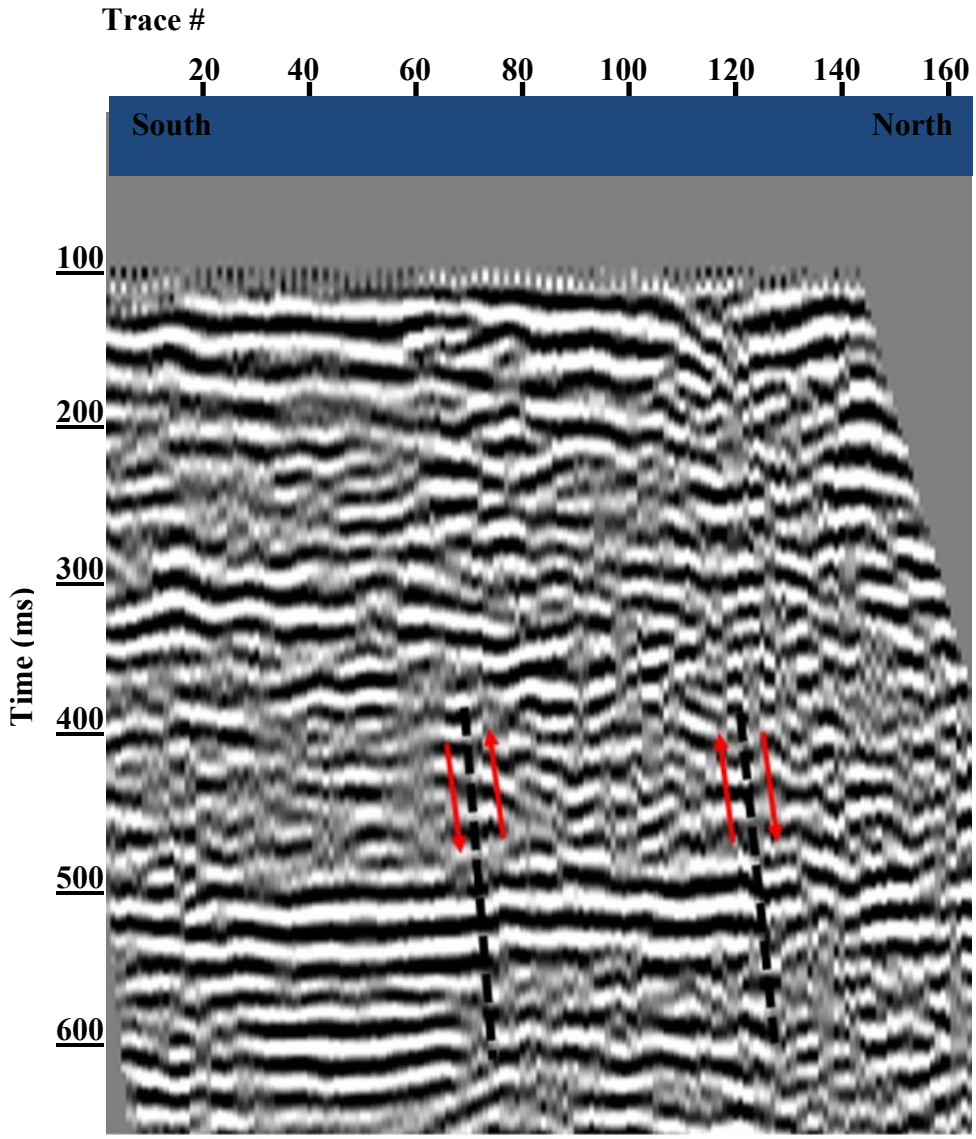

Figure 4.5. CUSSO 1 fault interpretations. Faults one and two are between trace numbers 140 and 110 and 100 and 68, respectively. The trace spacing is 5 meters. The dashed black lines represent faults one and two, and red arrows represent the direction of movement across faults.

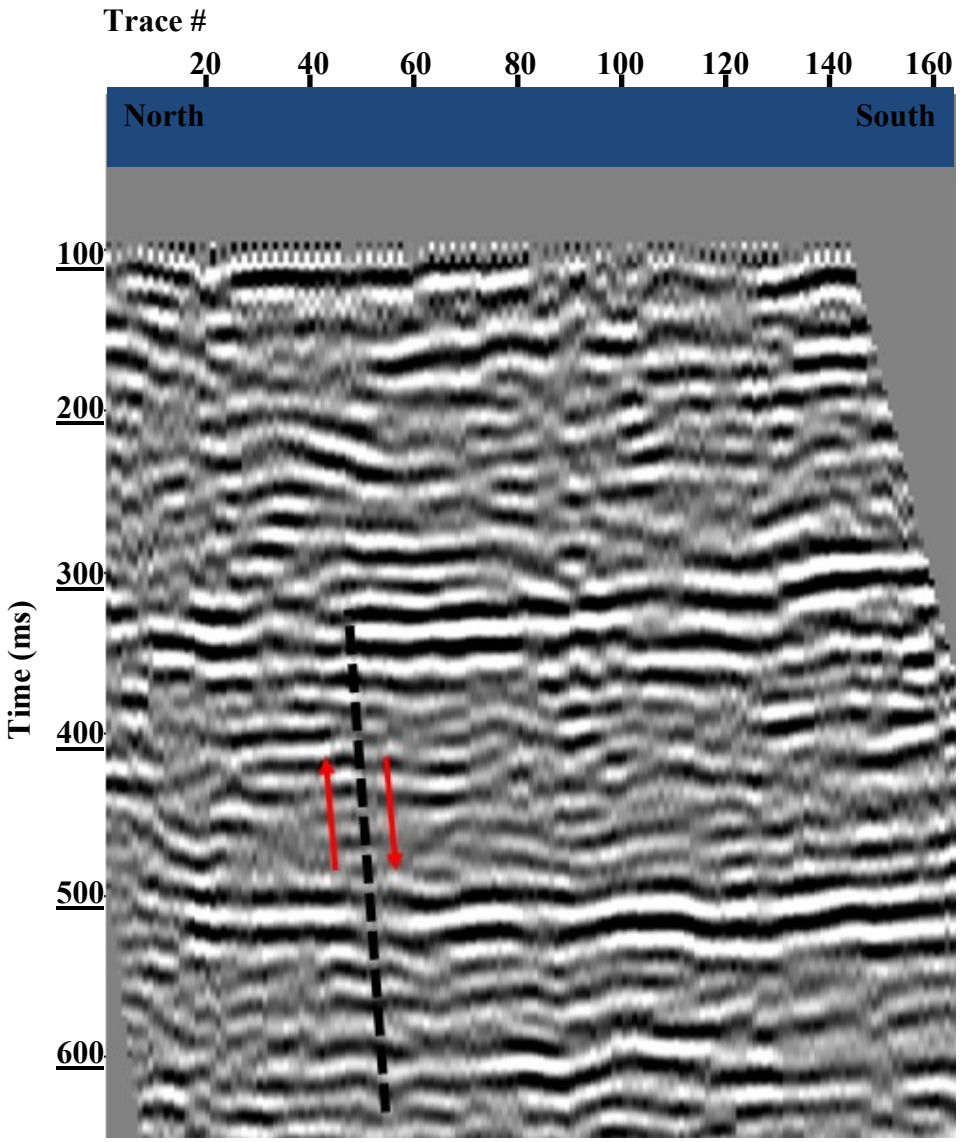

Figure 4.6. CUSSO 2 fault interpretation. Fault three is located between trace numbers 40 and 60. The trace spacing is 5 meters. The dashed black line represents fault three, and red arrows represent the direction of movement across faults.

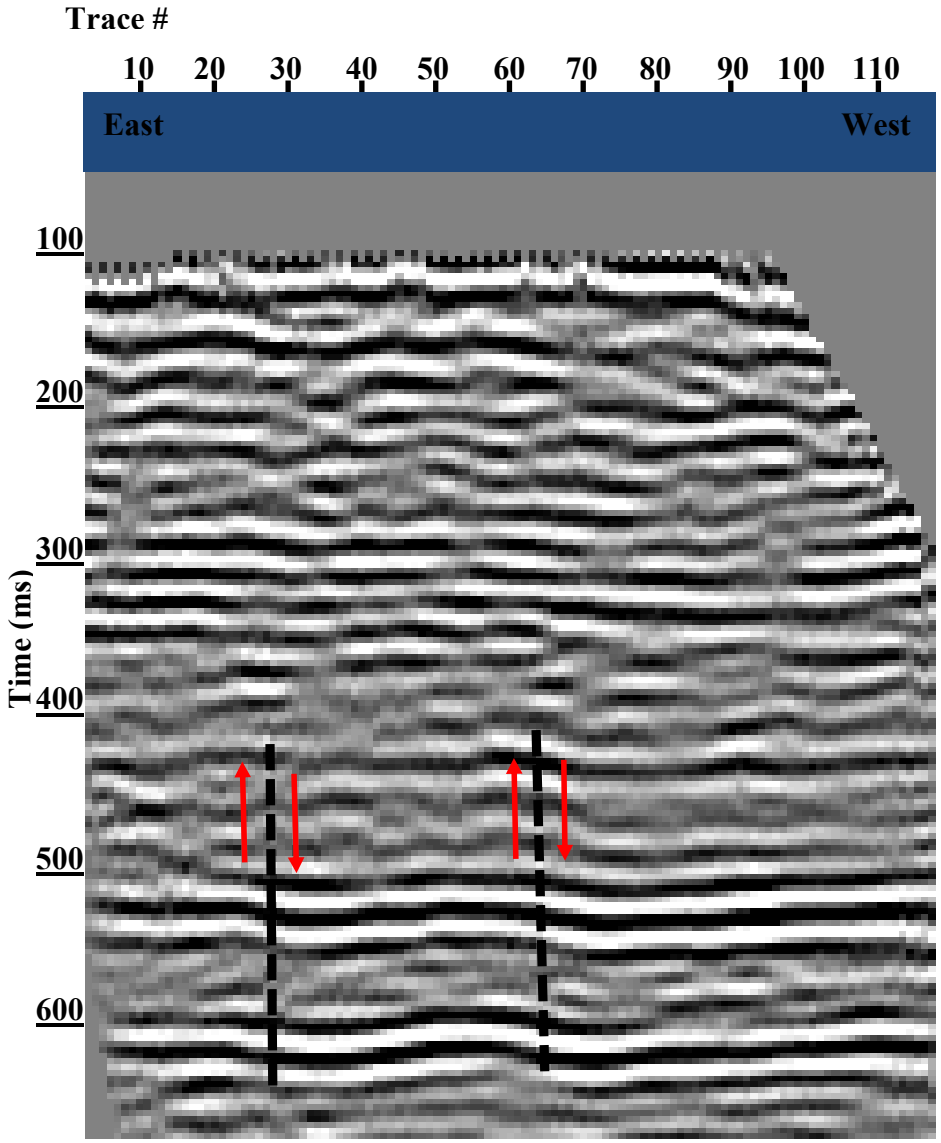

Figure 4.7. CUSSO 3 fault interpretations. Fault one is between trace numbers 50 and 70. Fault two is between trace numbers 20 and 30. The trace spacing is 5 meters. The dashed black lines represent faults one and two, and red arrows represent the direction of movement across faults.

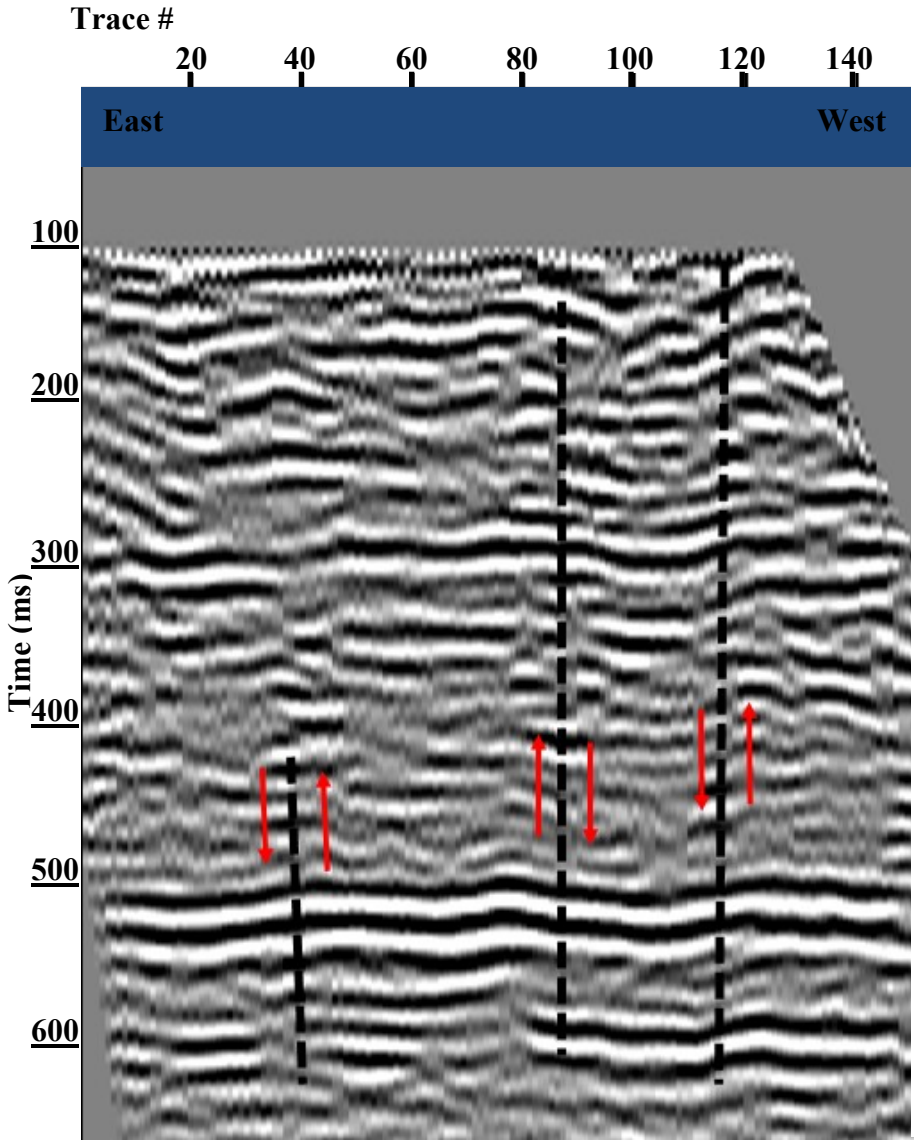

Figure 4.8. CUSSO 4 fault interpretations. Faults one and two occur between traces 80-89 and 37-48. The third interpreted fault is between traces 110-120 and may correlate with a larger structure between traces 80-120. The trace spacing is 5 meters. The dashed black lines represent faults one, two, and three, and red arrows represent the direction of movement across faults.

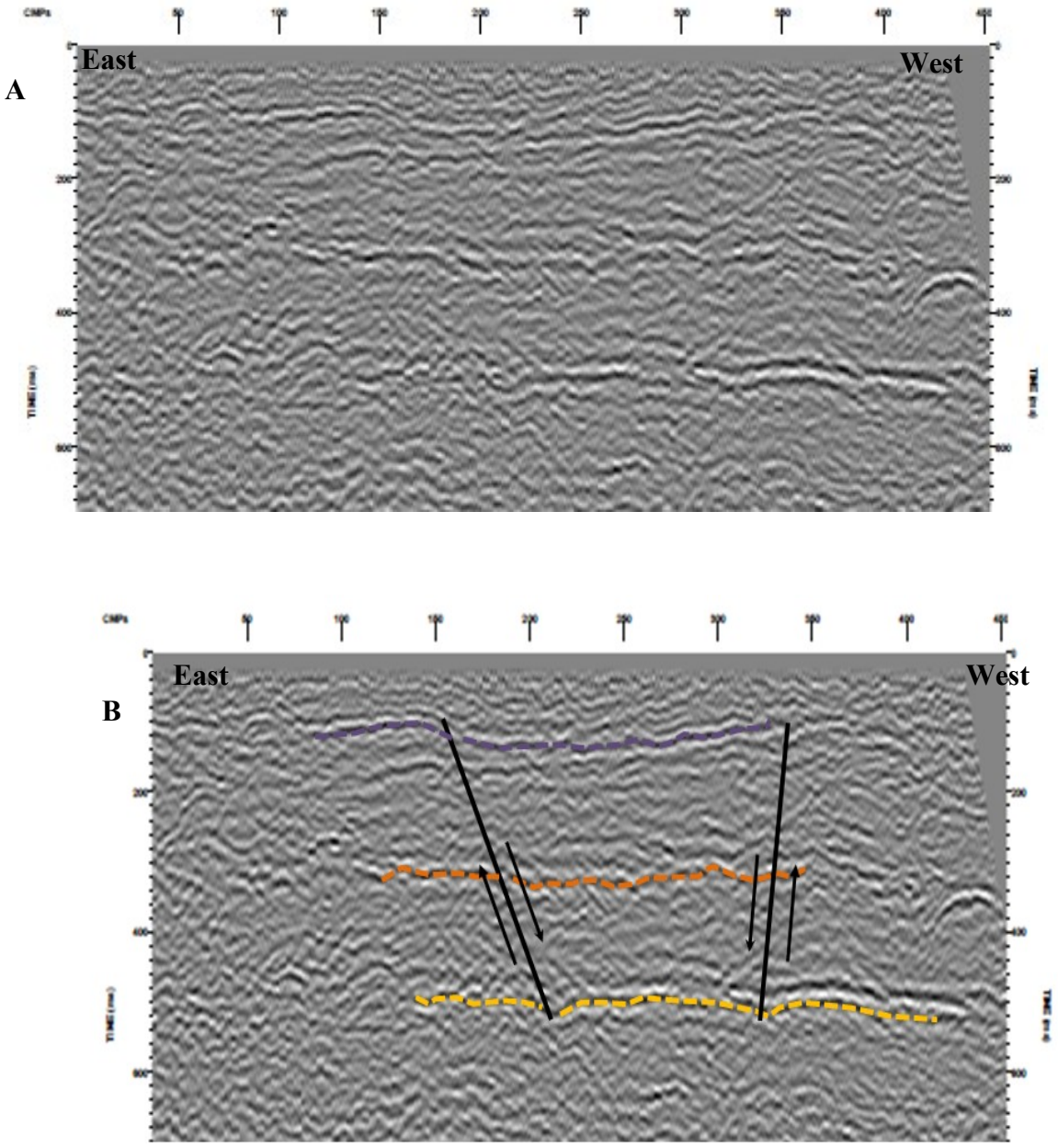

Figure 4.9. Uninterpreted (A) and interpreted (B) deformation zone along CUSSO 4. The three interpreted reflections are indicated by purple, orange, and yellow dotted lines.

CHAPTER FIVE: VELOCITY MAPS

5.1 Velocity Contour Maps

Velocity contour maps were created from three-component data (x,y, velocity) from CUSSO lines 1-6. All maps have a contour interval of 35 m/s and show depths of 10, 30, and 50 m. Artifacts seen on the three contour maps may be due to data gridding techniques. Figure (5.1-A) shows velocities at 10 m depth. Lower velocities at this depth are in the southeastern corner and, towards the northwest, the velocities begin to increase. Figure (5.1-B) shows velocities at 30 m depth. At this depth, velocity trends have changed from lower velocities in the southeast and higher to the northwest, to lower values in the northwest and higher to the southeast. Figure (5.1-C) shows velocities at 50 m depth and appears to have a similar velocity trend at 30 m depth. All three contour maps show an overall northeast-southwest velocity trend.

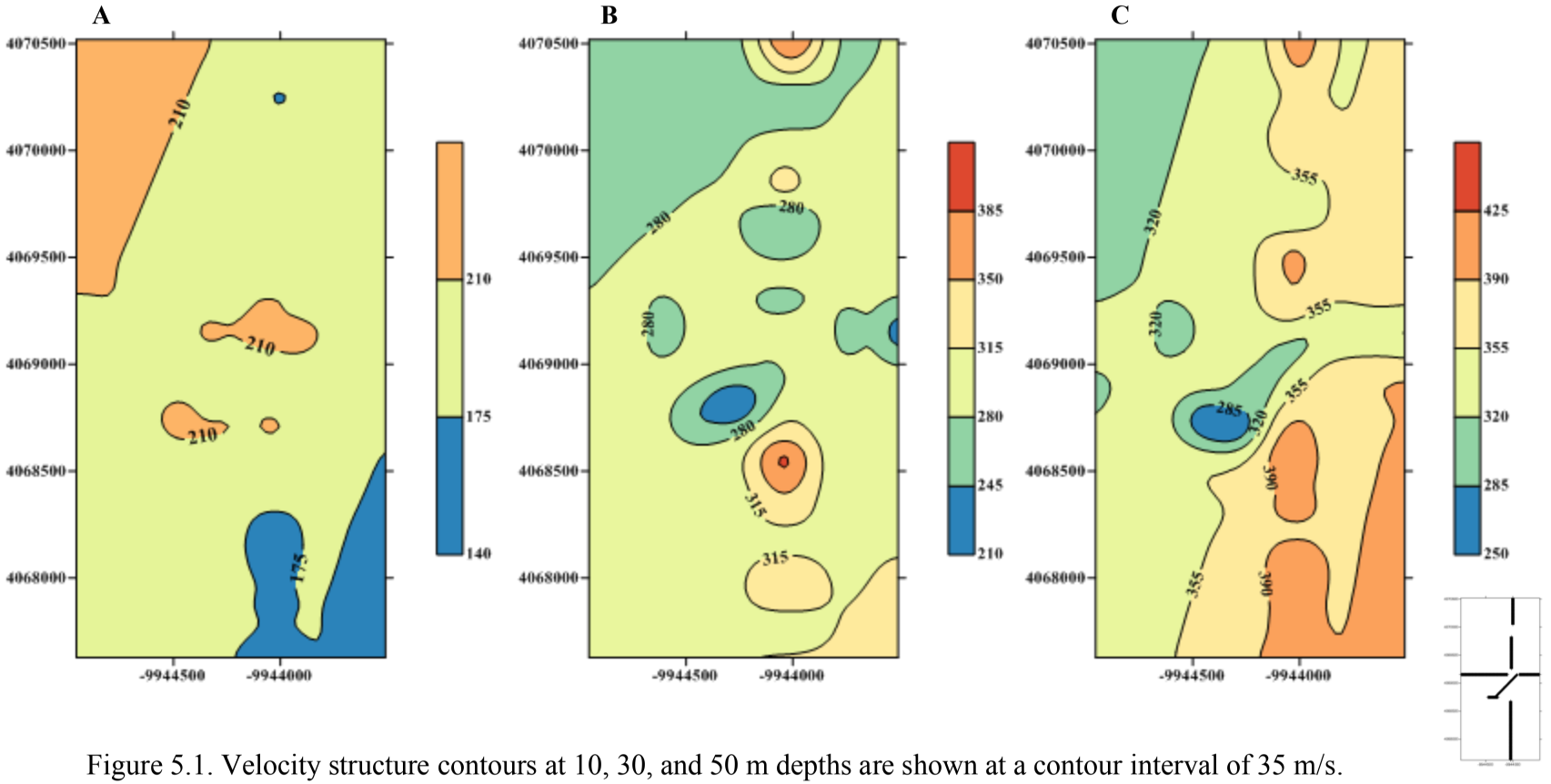

Figure 5.1. Velocity structure contours at 10, 30, and 50 m depths are shown at a contour interval of 35 m/s. (A) Velocity contours at 10 m depth. (B) Velocity contours at 30 m depth. (C) Velocity contours at 50 m depth. An index map for the CUSSO lines used in the creation of the contour maps is in the lower right corner. Circular artifacts seen on the three contour maps may be due to data gridding techniques. The overall trend of the data is northeast-southwest.

CHAPTER SIX: DISCUSSION

By using SH-wave refraction, three prominent seismic boundaries were characterized. The first and second layers correspond to Quaternary depths and the third correlates to the upper Eocene. Lithologic descriptions done by the Kentucky Geological Survey and the onsite borehole drillers report, support that layers one, two, and three correlate to fine sands, coarse sands/gravels, and unconsolidated clays, respectively. Although more work would need to be done in order to corroborate these lithologic descriptions.

SH-wave reflection resulted in three semicontinuous intervals. The seismic intervals corresponded with two Quaternary/upper Eocene layers and one upper to middle Eocene layer. These layers correlate in depth to the three SH-wave refraction layer and appear to have similar seismic velocities.

Six major seismic intervals were interpreted using reprocessed P-wave reflection data. These boundaries correlated with the Quaternary/Eocene, Eocene Jackson, Eocene Claiborne, Eocene Wilcox/Paleocene Porters Creek, Cretaceous McNairy and Paleozoic. The Quaternary and Eocene boundaries are better defined in the study although Hunter (2011) appears to have better layer resolution in the in the lower Eocene and Paleocene. Most of the other horizons remained at similar depths and perhaps, with additional data, the major seismic boundaries can be resolved with more detail.

The SH-wave refraction and P-and-SH reflection seismic models characterize major impedance boundaries in the 585 meters of Mississippi Embayment sediments at the CUSSO location. The major impedance boundaries described in this study are important in future ground motion modeling done at this location.

The faults imaged on seismic reflection profiles are striking northeast-southwest and agree with interpretations made by Hunter (2011). Faults, described northeast of the CUSSO location by Woolery et al. (2003), were interpreted to strike northeast-southwest and extend beneath the Mississippi Embayment sediment. Faults with similar trends were described in the area by Sexton and Jones (1986) and are likely due to common local stress patterns. The northeast-southwest trend is evident on most of the velocity contour maps and there does appear to be a subtle velocity difference associated with this interpreted fault trend.

The suspected deformation zone seen on the CUSSO 4 SH-wave reflection line does appear to have some degree of deformation in the near surface. The degree of layer resolution is such that the exact level of tectonics associated with this feature is inconclusive. To better image this structure, additional surveys over the zone will be needed. Refraction surveys may also be used to resolve suspected deformation features.

CHAPTER SEVEN: CONCLUSIONS

Understanding the Quaternary velocity model is an essential part of predicting earthquake ground motions at the Central United States Seismic Observatory. More than 4 km of SH-wave refraction/reflection and P-wave surveys were collected around the CUSSO borehole to better characterize seismic intervals from the Quaternary to the Paleozoic bedrock. All three complete velocity models (Figure 7.1) show major seismic intervals and velocities from the unconsolidated Quaternary sediments to the Paleozoic bedrock.

The 48 m of unconsolidated Quaternary sediments at CUSSO can have a significant influence on strong-motion characteristics such as amplitude, frequency, and duration. Nine refraction velocity models used to constrain Quaternary seismic intervals and included two Quaternary sections and one upper Eocene. The two quaternary intervals have an average velocity and thickness of 156 m/s and 262 m/s and 15 m and 30 m, respectively. The upper Eocene interval has a velocity of 386 m/s.

Five major reflectors were identified on the reprocessed CUSSO lines 1-4 and from those reflectors six stratigraphic zones were interpreted. The Quaternary/Eocene is located at depths between 0 and 90 m and the Eocene Jackson and is located between 90 and 145 m. The Eocene Claiborne is approximately between 145 and 295 m and the Eocene Wilcox/ Paleocene Porters Creek is interpreted to be between 295 and 512 meters. The Cretaceous McNairy is located between 512 and 625 m and the top of the Paleozoic bedrock is located at 625 m. The P-wave interval velocities associated with those intervals are 1482 m/s, 1761 m/s, 1797 m/s, 2182 m/s, and 2792 m/s, respectively.

The bedrock interval velocity could not be calculated, but according to the borehole P-wave velocity analysis, the bedrock velocity is near 3200 m/s.

Three semicontinuous reflectors were identified along the CUSSO 4 line. The first interval is located between 0 and 11m, the second between 11 and 66 m and the last between 66 and 202 m. The interval velocities associated with these zones are 184 m/s, 340 m/s, and 514 m/s respectively, and correlate to Quaternary, Quaternary/upper Eocene and middle to lower Eocene sediments, respectively. The three major impedance boundaries along the CUSSO 4 line, allowed for an additional connection between the refraction and reprocessed P-wave reflection velocity and depth data.

The majority of the high-angle faults appear to have a northeast-southwest trend and exhibit offset in the Paleozoic and Cretaceous horizons. Some faults are projected to extend into the Eocene and Paleocene, but offset at those horizons is not accurately resolvable.

The nearly 585 m of overburden that surrounds the Central United States Seismic Observatory varies horizontally and laterally throughout the Mississippi Embayment. The site models created from SH-wave refraction/reflection and P-wave reflection can be used to understand the complex sediment interactions between the Paleozoic bedrock and unconsolidated Quaternary.

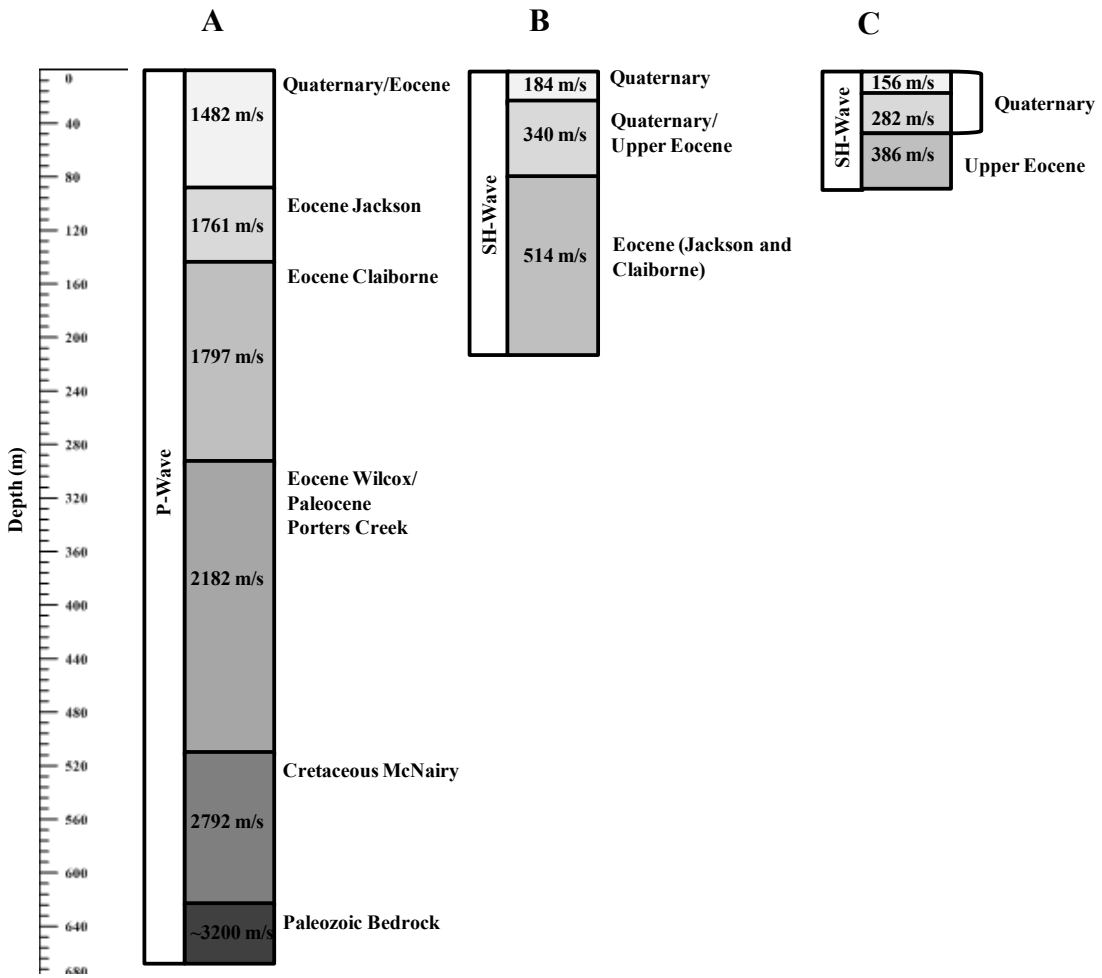

Figure 7.1. Major seismic intervals and velocities (m/s) associated with the three models. (A) Results of the reprocessed Hunter (2011) P-wave reflection lines. (B) Results of the SH-wave refraction analysis. (C) Results of the 4-m SH-wave reflection lines.

APPENDICES

APPENDIX A

Sounding Test CUSSO 2 (07/14/11)
Running Slough Road: N36°32'58.46" W89°19'43.95"
Filter: Lo 15 Hz High Off Notch 60 Hz
ΔT = .25 ms L = 1.024 s
Geophone spacing = 2 m

SH-Wave (30 Hz)

File	Stack	Location	Offset
7141101	+/-3	Geophone 1	-2 m North
7141102	+/-4	Geophone 1	-48 m North
7141103	+/-3	Geophone 24	none
7141104	+3	Geophone 24	none
7141105	-3	Geophone 24	none
7141106	+/-4	Geophone 48	+2 m South
7141107	+/- 4	Geophone 48	+48 m South

P-Wave (40 Hz)

File	Stack	Location	Offset
7141108	+4	Geophone 48	+2 m South
7141109	+7	Geophone 48	+48 m South
7141110	+4	Geophone 1	-2 m North
7141111	+7	Geophone 1	-48 m North
7141112	+12	Geophone 1	-96 m North

Sounding Test CUSSO 4 (07/15/11)
KY Hwy 971: N36° 33’ 13.69’’, W89° 19’45.54’’
Filter Lo 15 Hz High Off Notch 60 Hz
ΔT = .25 ms L = 1.024 s
Geophone spacing = 2 m

SH-Wave (30 Hz)

File	Stack	Location	Offset
7151101	+/-4	Geophone 1	-2 m North
7151102	+/-6	Geophone 1	-48 m North
7151103	+/-8	Geophone 1	-96 m North
7151104	+/-4	Geophone 24	none
7151105	+/-4	Geophone 48	+2 m South
7151106	+/-4	Geophone 48	+48 m South
7151107	+/-7	Geophone 48	+96 m South

P-Wave (40 Hz)

File	Stack	Location	Offset
7151108	+5	Geophone 48	+2 m North
7151109	+6	Geophone 48	+48 m North
7151110	+7	Geophone 48	+96 m North
7151111	+4	Geophone 1	-2 m South
7151112	+7	Geophone 1	-48 m South
7151113	+12	Geophone 1	-96 m South

Sounding Test CUSSO 3 (12/30/2011)
Chesshire Lane 36.55018, -89.33096 ~306 m
Filter Lo 15 Hz High Off
ΔT = .25 ms L = 1.024 s
Geophone spacing = 4 m

SH-Wave (30 Hz)

File	Stack	Location	Notes
12301101	±7	Geophone 1	N36.55021, W-89.33072 : No offset
12301102	±7	Geophone 12	No offset
12301103	±7	Geophone 24	No offset
12301104	±7	Geophone 36	No offset
12301105	±7	Geophone 48	N36.55032, W-89.33283: No offset

P-Wave (40 Hz)

File	Stack	Location
12301106	±7	Geophone 48
12301107	±7	Geophone 24
12301108	±7	Geophone 1

Sounding Test CUSSO 4 (12/31/2011)
Hwy. 971: N36° 33’ 13.69’’, W89° 19’45.54’’ 287 m
Filter Lo 15 Hz High Off
ΔT = .50 ms L = 1.024 s
Geophone spacing = 4 m

SH-Wave (30 Hz)

File	Stack	Location
1231101	±5	Geophone 1
1231102	±5	Geophone 12
1231102	±5	Geophone 24
1231103	±5	Geophone 36
1231104	±5	Geophone 48

P-Wave (40 Hz)

File	Stack	Location
1231106	±5	Geophone 48
1231107	±5	Geophone 24
1231108	±5	Geophone 1

P-Wave (40 Hz)

File	Stack	Location	Offset	Notes
1231109	?	Geophone 1		10 lb. Hammer
1231110	?	Geophone 1	-43.1 m East	Trigger Problems
1231111	?	Geophone 1	-43.1 m East	4 lb. Hammer
1231112	?	Geophone1		
1231113	?	Geophone 24		
1231114	?	Geophone 48		

CUSSO 4 (3/12/12)
Hwy. 971: N36° 33’ 13.69’’, W89° 19’45.54’’
Filter Lo 15 Hz High Off
ΔT = .50 ms L = 2 s
Geophone spacing = 10 m

SH-Wave (30 Hz)

File	Stack	Location
312101	+10/-15	Geophone 1
312102	±15	Geophone 12
312103	±15	Geophone 24
312104	±15	Geophone 36
312105	±15	Geophone 48

P-Wave (40 Hz)

File	Stack	Location
312201	±15	Geophone 48
312202	±15	Geophone 24
312203	±15	Geophone 1

CUSSO 4 (3/13/12)
CUSSO 4 Hwy. 971: N36° 33’ 13.69’’, W89° 19’45.54’’
Filter Lo 15 Hz High Off
ΔT = .50 ms L = 2 s
Geophone spacing = 4 m

SH-Wave (30 Hz)
First Segment

File	Stack	Location	Notes
313101	±7	Geophone 1	
313102	±10	Geophone 1	-48 m offset
313103	+5/-8	Geophone 12	
313104	±5	Geophone 24	
313105	±5	Geophone 36	
313106	±5	Geophone 48	
313107	±10	Geophone 48	+48 m offset

First 24 m Roll Along

File	Stack	Location	Notes
313108	+11/-10	Geophone 1	-48 m offset
313109	±5	Geophone 1	
3131010	±5	Geophone 12	*Geo 10 unplugged*
3131011	±5	Geophone 24	
3131012	±5	Geophone 36	
3131013	±5	Geophone 48	
3131014	±10	Geophone 48	+48 m offset

Second 24 m Roll Along

File	Stack	Location	Notes
3131015	±10	Geophone 1	-48 m offset
3131016	±5	Geophone 1	
3131017	±5	Geophone 12	
3131018	±5	Geophone 24	
3131019	±5	Geophone 36	
3131020	±5	Geophone 48	
3131021	±10	Geophone 48	+48 m offset

Third 24 m Roll Along

File	Stack	Location	Notes
3131022	±10	Geophone 1	-48 m offset
3131023	±5	Geophone 1	
3131024	±5	Geophone 12	
3131025	±5	Geophone 24	
3131026	±5	Geophone 36	
3131027	±5	Geophone 48	
3131028	±10	Geophone 48	+48 m offset

Fourth 24 m Roll Along

File	Stack	Location	Notes
3131029	±10	Geophone 1	-48 m offset
3131030	±5	Geophone 1	
3131031	±5	Geophone 12	
3131032	±5	Geophone 24	
3131033	±5	Geophone 36	
3131034	±5	Geophone 48	
3131035	±10	Geophone 48	+48 m offset

Fifth 24 m Roll Along

File	Stack	Location	Notes
3131036	±10	Geophone 1	-48 m offset
3131037	±5	Geophone 1	
3131038	±5	Geophone 12	
3131039	±5	Geophone 24	
3131040	±5	Geophone 36	
3131041	±5	Geophone 48	
3131042	±10	Geophone 48	+48 m offset

Sixth 24 m Roll Along

File	Stack	Location	Notes
3131043	±10	Geophone 1	-48 m offset
3131044	±5	Geophone 1	
3131045	±5	Geophone 12	
3131046	±5	Geophone 24	
3131047	±5	Geophone 36	
3131048	±5	Geophone 48	
3131049	±10	Geophone 48	+48 m offset

Seventh 24 m Roll Along

File	Stack	Location	Notes
3131050	±10	Geophone 1	-48 m offset
3131051	±5	Geophone 1	
3131052	±5	Geophone 12	
3131053	±5	Geophone 24	
3131054	±5	Geophone 36	
3131055	±5	Geophone 48	
3131056	±10	Geophone 48	+48 m offset

*** Geophone 48 is 91.7 m east of the last power pole on the left.

CUSSO 2 (3/14/12)
Running Slough Road: N36°32'58.46" W89°19'43.95"
Filter Lo 15 Hz High Off Notch 60 Hz
ΔT = .50 ms L = 2 s
Geophone spacing = 4 m
Notch Filter:60 Hz (Line runs parallel to powerlines)

SH-Wave (30 Hz)
First Segment

File	Stack	Location	Notes
314101	±10	Geophone 1	-48 m offset
314102	±5	Geophone 1	
314103	±5	Geophone 12	
314104	±5	Geophone 24	
314105	±5	Geophone 36	
314106	±5	Geophone 48	
314107	±10	Geophone 48	+48 m offset

First 24 m Roll Along

File	Stack	Location	Notes
314108	±10	Geophone 1	-48 m offset
314109	±5	Geophone 1	
314110	±5	Geophone 12	
314111	±5	Geophone 24	
314112	±5	Geophone 36	
314113	±5	Geophone 48	
314114	±10	Geophone 48	+48 m offset

Second 24 m Roll Along

File	Stack	Location	Notes
314115	±10	Geophone 1	-48 m offset
314116	±5	Geophone 1	
314117	±5	Geophone 12	
314118	±5	Geophone 24	
314119	±5	Geophone 36	
314120	±5	Geophone 48	
314121	±10	Geophone 48	+48 m offset

Third 24 m Roll Along

File	Stack	Location	Notes
314122	±10	Geophone 1	-48 m offset
314123	±5	Geophone 1	
314124	±5	Geophone 12	
314125	±5	Geophone 24	
314126	±5	Geophone 36	
314127	±5	Geophone 48	
314128	±10	Geophone 48	+48 m offset

Fourth 24 m Roll Along

File	Stack	Location	Notes
314129	±10	Geophone 1	-48 m offset
314130	±5	Geophone 1	
314131	±5	Geophone 12	
314132	±5	Geophone 24	
314133	±5	Geophone 36	
314134	±5	Geophone 48	
314135	±10	Geophone 48	+48 m offset

Fifth 24 m Roll Along

File	Stack	Location	Notes
314136	±10	Geophone 1	-48 m offset
314137	±5	Geophone 1	
314138	±5	Geophone 12	
314139	±5	Geophone 24	
314140	±5	Geophone 36	
314141	±5	Geophone 48	
314142	±10	Geophone 48	+48 m offset

Sixth 24 m Roll Along

File	Stack	Location	Notes
314143	±10	Geophone 1	-48 m offset
314144	±5	Geophone 1	
314145	±5	Geophone 12	
314146	±5	Geophone 24	
314147	±5	Geophone 36	
314148	±5	Geophone 48	
314149	±10	Geophone 48	+48 m offset

Seventh 24 m Roll Along

File	Stack	Location	Notes
314150	±10	Geophone 1	-48 m offset
314151	±5	Geophone 1	
314152	±5	Geophone 12	
314153	±5	Geophone 24	
314154	±5	Geophone 36	
314155	±5	Geophone 48	
314156	±10	Geophone 48	+48 m offset

Eighth 24 m Roll Along

File	Stack	Location	Notes
314157	±10	Geophone 1	-48 m offset
314158	±5	Geophone 1	
314159	±5	Geophone 12	
314160	±5	Geophone 24	
314161	±5	Geophone 36	
314162	±5	Geophone 48	
314163	+10/-9	Geophone 48	+48 m offset

Ninth 24 m Roll Along

File	Stack	Location	Notes
314164	±10	Geophone 1	-48 m offset
314165	±5	Geophone 1	+4/-5
314166	±5	Geophone 12	
314167	±5	Geophone 24	
314168	±5	Geophone 36	
314169	±5	Geophone 48	
314170	±10	Geophone 48	+48 m offset

CUSSO 1 (4/16/2012)
CUSSO 1 Sassafrass Church Road N36° 33' 17.23", W-89°19'43.42"
Filter Lo 15 Hz High Off Notch 60 Hz
ΔT = .50 ms L = 2 s
Notch Filter:60 Hz (Line runs parallel to powerlines)
Geophone spacing = 4 m

SH-Wave (30 Hz)
Line 1-A First 48 geophones

Field File	Location	Stack	Notes
462101	Geophone 1	± 10	-48 m Offset
462102	Geophone 1	± 5	
462103	Geophone 12	± 5	
462104	Geophone 24	± 5	
462105	Geophone 36	± 5	
462106	Geophone 48	± 5	
462107	Geophone 48	± 10	+48 m Offset

Line 1-A First 24 m Roll Along

Field File	Location	Stack	Notes
462108	Geophone 1	± 10	-48 m Offset
462109	Geophone 1	± 5	Plane Flying
462110	Geophone 12	± 5	Plane Flying
462111	Geophone 24	± 5	Plane Flying
462112	Geophone 36	± 5	Plane Flying
462113	Geophone 48	± 5	Plane Flying
462114	Geophone 48	± 10	+ 48m Offset (culvert)

Line 1-A Second 24 m Roll Along

Field File	Location	Stack	Notes
462115	Geophone 1	± 10	-48 m Offset (Battery Change)
462116	Geophone 1	± 5	
462117	Geophone 12	± 5	
462118	Geophone 24	± 5	
462119	Geophone 36	± 5	
462120	Geo phone48	± 5	
462121	Geophone 48	± 10	+48 m Offset (culvert)

***** Geo 25-27 gravel (coupling not great)

Line 1-A Third 24 m Roll Along

Field File	Location	Stack	Notes
462122	Geophone 1	± 10	-48 m Offset
462123	Geophone 1	± 5	
462124	Geophone 12	± 5	
462125	Geophone 24	± 5	
462126	Geophone 36	± 5	
462127	Geophone 48	± 5	
462128	Geophone 48	± 10	+48 m Offset

*122 Polarity started negative and finished positive (reversed).

Line 1-A Fourth 24 m Roll Along

Field File	Location	Stack	Notes
462129	Geophone 1	± 10	-48 m Offset
462130	Geophone 1	+5 / -6	
462131	Geophone12	± 5	
462132	Geophone 24	± 5	
462133	Geophone 36	± 5	
462134	Geophone 48	± 5	
462135	Geophone 48	± 10	+48 m Offset

***** 462135 is located in front of the white barn.

Line 1-B

First Segment 24 m Roll Along (5th)

136 start: 36°33'40.63" -89°19'42.60" (462135 + 56m)

Field File	Geophone	Stack	Notes
462136	Geophone 1	± 10	-48 m Offset
462137	Geophone 1	+5 / -6	
462138	Geophone 12	± 5	
462139	Geophone 24	± 5	
462140	Geophone 36	± 5	
462141	Geophone 48	± 5	
462142	Geophone 48	± 10	+48 m Offset

Line 1-B First Roll Along 24 m Roll Along (6th)

Field File	Geophone	Stack	Notes
462143	Geophone 1	± 10	-48 m Offset
462144	Geophone 1	± 5	
462145	Geophone 12	± 5	
462146	Geophone 24	± 5	
462147	Geophone 36	± 5	*Geo 34 power line*
462148	Geophone 48	± 5	
462149	Geophone 48	± 10	+48 m Offset

Line 1-B Second Roll Along 24 m Roll Along (7th)

Field File	Geophone	Stack	Notes
462150	Geophone 1	± 10	-48 m Offset
462151	Geophone 1	± 5	
462152	Geophone 12	± 5	
462153	Geophone 24	± 5	
462154	Geophone 36	± 5	
462155	Geophone 48	± 5	
462156	Geophone 48	± 10	+48 m Offset

Line 1-B Third Roll Along 24 m Roll Along (8th)

Field File	Geophone	Stack	Notes
462157	Geophone 1	± 10	-48 m Offset
462158	Geophone 1	± 5	
462159	Geophone 12	± 5	
462160	Geophone 24	± 5	
462161	Geophone 36	± 5	
462162	Geophone 48	± 5	
462163	Geophone 48	± 10	+48 m Offset

CUSSO 5 (6/20/2012)
Highway 94: N36°33.226', W89°19.667'
Filter Lo 15 Hz High Off Notch 60 Hz
ΔT = .25 ms L = 1.24 s
Geophone Spacing (4 m)

SH-Wave (30 Hz)

File	Stack	Location	Offset
6202101	+/-9	Geophone 1	-48 m
6202102	+6/-5	Geophone 1	None
6202103	+/-5	Geophone 12	None
6202104	+/-5	Geophone 24	None
6202105	+/-5	Geophone 36	None
6202106	+/-10	Geophone 48	None
6202107	+/-10	Geophone 48	+48 m

First 24 m Roll Along

File	Stack	Location	Offset
6202108	+/-10	Geophone 1	-48 m
6202109	+/-10	Geophone 1	None
6202110	+/-5	Geophone 12	None
6202111	+/-5	Geophone 24	None
6202112	+/-5	Geophone 36	None
6202113	+/-10	Geophone 48	None
6202114	+/-10	Geophone 48	+48 m

Second 24 m Roll Along

File	Stack	Location	Offset
6202115	+/-10	Geophone 1	-48 m
6202116	+/-10	Geophone 1	None
6202117	+/-5	Geophone 12	None
6202118	+/-5	Geophone 24	None
6202119	+/-5	Geophone 36	None
6202120	+/-10	Geophone 48	None
6202121	+/-10	Geophone 48	+48 m

CUSSO 6 (6/21/2012)
Cotton Gin Road: N36°33.229', W89°19.648'
Filter Lo 15 Hz High Off Notch 60 Hz
ΔT = .25 ms L = 1.24 s
Geophone Spacing (4 m)

SH-Wave (30 Hz)

File	Stack	Location	Offset
6202201	+/-10	Geophone 1	-48 m
6202202	+/-10	Geophone 1	None
6202203	+/-5	Geophone 12	None
6202204	+/-5	Geophone 24	None
6202205	+/-5	Geophone 36	None
6202206	+/-10	Geophone 48	None
6202207	+/-10	Geophone 48	+48 m

First 24 m Roll Along

File	Stack	Location	Offset
6202208	+/-10	Geophone 1	-48 m
6202209	+/-10	Geophone 1	None
6202210	+/-5	Geophone 12	None
6202211	+/-5	Geophone 24	None
6202212	+/-5	Geophone 36	None
6202213	+/-10	Geophone 48	None
6202214	+/-10	Geophone 48	+48 m

Second 24 m Roll Along

File	Stack	Location	Offset
6202215	+/-10	Geophone 1	-48 m
6202216	+/-10	Geophone 1	None
6202217	+/-5	Geophone 12	None
6202218	+/-5	Geophone 24	None
6202219	+/-5	Geophone 36	None
6202220	+/-10	Geophone 48	None
6202221	+/-10	Geophone 48	+48 m

APPENDIX B

CUSSO 4 Reflection Line (7/12/12)

CUSSO 4 Hwy. 971: N36° 33’ 13.69’’, W89° 19’45.54’’
Filter Lo 15 Hz High Off
ΔT = .50 ms L = 2 s
Geophone spacing = 2 m

1st Section (Ji Wei Hitter) **2nd Section (Ali and Dr. Woolery Hitters)**

File	Stack	Location	File	Stack	Location
712101	± 3	Geophone 1	712125	± 3	Geophone 1
712102	± 3	Geophone 2	712126	± 3	Geophone 2
712103	± 3	Geophone 3	712127	± 3	Geophone 3
712104	± 3	Geophone 4	712128	± 3	Geophone 4
712105	± 3	Geophone 5	712129	± 3	Geophone 5
712106	± 3	Geophone 6	712130	± 3	Geophone 6
712107	± 3	Geophone 7	712131	± 3	Geophone 7
712108	± 3	Geophone 8	712132	± 3	Geophone 8
712109	± 3	Geophone 9	712133	± 3	Geophone 9
712110	± 3	Geophone 10	712134	± 3	Geophone 10
712111	± 3	Geophone 11	712135	± 3	Geophone 11
712112	± 3	Geophone 12	712136	± 3	Geophone 12
712113	± 3	Geophone 13	712137	± 3	Geophone 13
712114	± 3	Geophone 14	712138	± 3	Geophone 14
712115	± 3	Geophone 15	712139	± 3	Geophone 15
712116	± 3	Geophone 16	712140	± 3	Geophone 16
712117	± 3	Geophone 17	712141	± 3	Geophone 17
712118	± 3	Geophone 18	712142	± 3	Geophone 18
712119	± 3	Geophone 19	712143	± 3	Geophone 19
712120	± 3	Geophone 20	712144	± 3	Geophone 20
712121	± 3	Geophone 21	712145	± 3	Geophone 21
712122	± 3	Geophone 22	712146	± 3	Geophone 22
712123	± 3	Geophone 23	712147	± 3	Geophone 23
712124	± 3	Geophone 24	712148	± 3	Geophone 24

3rd Section (Carrington Hitter) 4th Section (Ali Hitter)

File	Stack	Location	File	Stack	Location
712149	± 3	Geophone 1	712173	± 3	Geophone 1
712150	± 3	Geophone 2	712174	± 3	Geophone 2
712151	± 3	Geophone 3	712175	± 3	Geophone 3
712152	± 3	Geophone 4	712176	± 3	Geophone 4
712153	± 3	Geophone 5	712177	± 3	Geophone 5
712154	± 3	Geophone 6	712178	± 3	Geophone 6
712155	± 3	Geophone 7	712179	± 3	Geophone 7
712156	± 3	Geophone 8	712180	± 3	Geophone 8
712157	± 3	Geophone 9	712181	± 3	Geophone 9
712158	± 3	Geophone 10	712182	± 3	Geophone 10
712159	± 3	Geophone 11	712183	± 3	Geophone 11
712160	± 3	Geophone 12	712184	+3/-4	Geophone 12
712161	± 3	Geophone 13	712185	± 3	Geophone 13
712162	± 3	Geophone 14	712186	± 3	Geophone 14
712163	± 3	Geophone 15	712187	± 3	Geophone 15
712164	± 3	Geophone 16	712188	± 3	Geophone 16
712165	± 3	Geophone 17	712189	± 3	Geophone 17
712166	± 3	Geophone 18	712190	± 3	Geophone 18
712167	± 3	Geophone 19	712191	± 3	Geophone 19
712168	± 3	Geophone 20	712192	± 3	Geophone 20
712169	± 3	Geophone 21	712193	± 3	Geophone 21
712170	± 3	Geophone 22	712194	± 3	Geophone 22
712171	± 3	Geophone 23	712195	± 3	Geophone 23
712172	± 3	Geophone 24	712196	± 3	Geophone 24

**** Notes** Perhaps 172 did not get saved, so restart on next line (offset 2 m, on last geophone)**

**** Notes ** Culvert from 184-187**

5th Section (Ji Wei Hitter) **6th Section (Carrington Hitter)**

File	Stack	Location	File	Stack	Location
712197	± 3	Geophone 1	712221	± 3	Geophone 1
712198	± 3	Geophone 2	712222	± 3	Geophone 2
712199	± 3	Geophone 3	712223	± 3	Geophone 3
712200	± 3	Geophone 4	712224	± 3	Geophone 4
712201	± 3	Geophone 5	712225	± 3	Geophone 5
712202	± 3	Geophone 6	712226	± 3	Geophone 6
712203	± 3	Geophone 7	712227	± 3	Geophone 7
712204	± 3	Geophone 8	712228	± 3	Geophone 8
712205	± 3	Geophone 9	712229	± 3	Geophone 9
712206	+3/-4	Geophone 10	712230	± 3	Geophone 10
712207	± 3	Geophone 11	712231	± 3	Geophone 11
712208	± 3	Geophone 12	712232	± 3	Geophone 12
712209	± 3	Geophone 13	712233	± 3	Geophone 13
712210	± 3	Geophone 14	712234	± 3	Geophone 14
712211	± 3	Geophone 15	712235	± 3	Geophone 15
712212	± 3	Geophone 16	712236	± 3	Geophone 16
712213	± 3	Geophone 17	712237	± 3	Geophone 17
712214	± 3	Geophone 18	712238	± 3	Geophone 18
712215	± 3	Geophone 19	712239	± 3	Geophone 19
712216	± 3	Geophone 20	712240	± 3	Geophone 20
712217	± 3	Geophone 21	712241	± 3	Geophone 21
712218	± 3	Geophone 22	712242	± 3	Geophone 22
712219	± 3	Geophone 23	712243	± 3	Geophone 23
712220	± 3	Geophone 24	712244	± 3	Geophone 24

**** Notes ** Ji Wei is hitter from 197-210, Olivia from 210-211, and Li is hitter from 212-220. Three good reflections around 160, 200, and 360 ms.**

**** Notes ** File 237 was a double save?**

(7/13/12)

7th Section (Ji Wei Hitter) **8th Section (Ali Hitter)**

File	Stack	Location	File	Stack	Location
712245	± 3	Geophone 1	712269	± 3	Geophone 1
712246	± 3	Geophone 2	712270	± 3	Geophone 2
712247	± 3	Geophone 3	712271	± 3	Geophone 3
712248	± 3	Geophone 4	712272	± 3	Geophone 4
712249	± 3	Geophone 5	712273	± 3	Geophone 5
712250	± 3	Geophone 6	712274	± 3	Geophone 6
712251	± 3	Geophone 7	712275	± 3	Geophone 7
712252	± 3	Geophone 8	712276	± 3	Geophone 8
712253	± 3	Geophone 9	712277	± 3	Geophone 9
712254	± 3	Geophone 10	712278	± 3	Geophone 10
712255	± 3	Geophone 11	712279	± 3	Geophone 11
712256	± 3	Geophone 12	712280	± 3	Geophone 12
712257	± 3	Geophone 13	712281	± 3	Geophone 13
712258	± 3	Geophone 14	712282	± 3	Geophone 14
712259	± 3	Geophone 15	712283	± 3	Geophone 15
712260	± 3	Geophone 16	712284	± 3	Geophone 16
712261	± 3	Geophone 17	712285	± 3	Geophone 17
712262	± 3	Geophone 18	712286	± 3	Geophone 18
712263	± 3	Geophone 19	712287	± 3	Geophone 19
712264	± 3	Geophone 20	712288	± 3	Geophone 20
712265	± 3	Geophone 21	712289	± 3	Geophone 21
712266	± 3	Geophone 22	712290	± 3	Geophone 22
712267	± 3	Geophone 23	712291	± 3	Geophone 23
712268	± 3	Geophone 24	712292	± 3	Geophone 24

9th Section (Carrington Hitter)

File	Stack	Location
712293	± 3	Geophone 1
712294	± 3	Geophone 2
712295	± 3	Geophone 3
712296	± 3	Geophone 4
712297	± 3	Geophone 5
712298	± 3	Geophone 6
712299	± 3	Geophone 7
712300	± 3	Geophone 8
712301	± 3	Geophone 9
712302	± 3	Geophone 10
712303	± 3	Geophone 11
712304	± 3	Geophone 12
712305	± 3	Geophone 13
712306	± 3	Geophone 14
712307	± 3	Geophone 15
712308	± 3	Geophone 16
712309	± 3	Geophone 17
712310	± 3	Geophone 18
712311	± 3	Geophone 19
712312	± 3	Geophone 20
712313	± 3	Geophone 21
712314	± 3	Geophone 22
712315	± 3	Geophone 23
712316	± 3	Geophone 24

**** Notes ** Ji Wei hit from 310-316**

**** Notes ** Last Geophone 4.5 m from center of culvert**

APPENDIX C

Processing Procedures (Extended)

1. Reformat from DAT to internal Vista format
2. Input geometry
3. Time variant scaling
    a. Scale: 1.0 RMS Trim Median
    b. Window Type: Dynamic
    c. SC Interpolation: Logarithmic
    d. Define Time Window by User Defined Time Windows
        1: S: 0.0 E: 100.0 A: 50.0
        2: S: 50.0 E: 150.0 A: 100.0
        3: S 100.0 E: 300.0 A: 200.0
        4: S 200.0 E: 400.0 A: 300.0
        5: S 300.0 E:500.0 A: 400.0
        6: S 400.0 E: 600.0 A: 500.0
4. Data Scaling
    a. Scale: 1.0 Mean Scale
    b. Gate Window: Entire Trace
5. Ormsby Band-Pass Filter
    a. 15/25-70/80 Hz
6. Data Scaling
    a. Scale: 1.0 Mean Scale
    b. Gate Window: Entire Trace
7. Mute Traces
    a. Taper Mute Zones by 4 Samples
8. FK-Filter
    a. Power: 1.0
    b. Trace Smooth: 7
    c. Frequency Smooth: 5
9. Adaptive Subtraction (Multiple Attenuation)
    a. Time Domain Adaptive Subtraction
    b. Operator Lag: 10.0 ms Moving Window Shift: 80%
    c. Output: Subtraction
    d. Start Time: 50.0 ms End Time: 1024.0 ms
    e. Start Time Defined by NMO Velocity: 300.0 m/s
    f. Operator Len: 25.0 ms
    g. Pre-Whitening: 2.0% Moving Window: 300.0
10. Surface Consistence Deconveloution
    a. Type: Spiking Deconveloution
    b. Operator Length: 80.0
    c. Pre-Whitening: 1.0
11. Normal Move-out
12. Threshold Median Noise Attenuation
    a. Window Length: 75.0 ms
    b. N CDPs to Smash: 3
    c. Median Length: 13
    d. Attenuation Multiplier: 3.0
    e. Min Apply Frequency: 0.0 Hz Max Apply Frequency: 100.0 Hz

f. Sort Super-Gather by offset
g. Threshold – Frequency: 30.0 Amplitude: 2.5

13. Common Mid-Points Stack
    a. CMP Stack Geometry Header Update: ON
14. Deconvolution
    a. Type: Spiking Deconvolution
    b. Operator Length: 100.0 ms
    c. Apply Operator Taper: 10.0 ms
    d. Pre-Whitening: 1.0
    e. Gate Window: Entire Trace

BIBLIOGRAPHY

Abd-Aal, A.K., and Mohamed, A.A. (2009). Near-surface seismic refraction applied to exploring subsurface clay layer at a new mining area in southeast Cairo, Egypt, Arabian Journal of Geoscience, 3, 105-112.

Bolt, B.A. (2003). Earthquakes, Fifth Edition. New York, W.H. Freeman and Company, 320.

Bickford, M.E., Van Schmus, W.R., Macdonald, R., Lewry, T.F., and Pearson, J.G. (1986). U-Pb zircon geochronology project for the Trans-Hudson Orogen: Current sampling and recent results; in Summary of Investigations, Saskatchewan Geological Survey, Saskatchewan Energy and Mines, Miscellaneous Report 86-84, 101-107.

Braile, L.W., Hinze, W.J., Keller, G.R., Lidiak, E.G., and Sexton, J.L. (1986). Tectonic development of the New Madrid complex, Mississippi Embayment: North America, Tectonophysics, 131, 1–21.

Chiemeke, C.C., and Osazwa, I.B. (2009). An improved technique for static correction in high resolution shallow seismic reflection data using difference in reflection times, Journal of the Environment, 5, 72-79.

Conrad, T. A. (1847). Observations on the Eocene formation, and descriptions of one hundred and five new fossils of that period, from the vicinity of Vicksburg, Mississippi, with an appendix. Proceedings of the Academy of Natural Sciences of Philadelphia. 3, 280-299.

Cox, R.T., and Van Arsdale, R.B. (1997). Hotspot origin of the Mississippi Embayment and its possible impact on contemporary seismicity, Engineering Geology, 46, 201–206.

Cox, R.T., and Van Arsdale, R.B. (2002). The Mississippi Embayment, North America: A first order continental structure generated by the Cretaceous superplume mantle event, Journal of Geodynamics, 34, 163–176.

Csontos, R., Van Arsdale, R., Cox, R., and Waldron, B. (2008). The Reelfoot Rift and its impact on Quaternary deformation in the central Mississippi River Valley, Geosphere, 4, 145-158.

Dart, R.L., and Swolfs, H.S. (1998). Contour mapping of relic structures in the Precambrian basement of the Reelfoot Rift: North American Midcontinent, Tectonics, 17, 235–249.

Diabiase, R. (2004). Seismic refraction analysis of sediment fill in cyclone graben, needles district canyonlands national park, Eighteenth Annual Keck Research Symposium in Geology Proceedings, 11.

Drahovzal, J.A., Harris, D.C., Wickstrom, L.H., Walker, D., Baranoski, M.T., Keith, B., and Furer, L.C. (1992). The East Continent Rift Basin: A new discovery, Kentucky Geological Survey Special Publication 18, 25.

Easson, G.L., F. Faruque and L.D. Yarbrough, 2005, Rating the Shrink/Swell Behavior of the Porters Creek Formation, Environmental & Engineering Geoscience, 11, 171–176.

Ervin, C. P, and McGinnis, L.D. (1975). Reelfoot Rift-Reactivated precursor to the Mississippi Embayment, Geological Society of American Bulletin, 86, 1287–1295.

Hilgard, E.W. (1860). Report on geology and agriculture of the state of Mississippi, 128-135.

Geldart, L.P., and Sheriff, R.E. (2004). Problems in exploration seismology and their solutions, Tulsa, Society of Exploration Geophysicists, 514.

GeoVision Geophysical Services. (2007). Draft report CUSSO boring geophysical logging, .

Gregory, L.E., Fazlay., F., and Yarbrough., L.D. (2005). Rating the shrink/swell behavior of the Porters Creek Formation, Environmental & Engineering Geoscience, 11, 171-176.

Heigold, P.C., and Kolata, D.R. (1993). Proterozoic crustal boundary in the southern part of the Illinois Basin, Tectonophysics, 217, 307–319.

Hendricks, J.D. (1988). Bouguer gravity of Arkansas, U.S. Geological Survey, Professional Paper, 1474,31.

Hildenbrand, T.G. (1985). Rift structure of the northern Mississippi Embayment from the analysis of gravity and magnetic data, Journal of Geophysical Research, 90, 12607–12622.

Howe, J.R., and Thompson, T.L. (1984). Tectonics, sedimentation, and hydrocarbon potential of the Reelfoot Rift, Oil and Gas Journal, 82, 179–190.

Hunter, D. (2011). Defining the geologic site model for the Central United States Seismic Observatory. University of Kentucky, Lexington, Ky.

Kane, M. F., Hildenbrand, T.G., and Hendricks, J.D. (1981). Model for the tectonic evolution of the Mississippi Embayment and its contemporary seismicity, Geology 9, 563–568.

Keller, G., D'Hondt, S., and Vallier, T.L. (1983). Multiple microtektite horizons in upper Eocene marine sediments: No evidence of mass extinctions, Science 221, 150-152.

Kelson, K. I., Simpson, G. D., Lettis, W. R., and Haraden, C. C. (1996). Holocene slip rate and recurrence of the Northern Calaveras Fault at Leyden Creek, eastern San Francisco Bay region, Journal of Geophysical Research, 101, 5961-5975.

Kolata, D.R., and Nelson, W.J. (1991). Tectonic history of the Illinois Basin, in Leighton, M.W., Kolata, D.R., Oltz, D.F., and Eidel, J.J. eds., Interior cratonic basins, American Association of Petroleum Geologists Memoir, 51, 263–285.

Mayne, W.H. (1962). Common reflection point horizontal data stacking T\techniques, Geophysics, 27, 927−938.

Mooney, W.D., Andrews, M.C., Ginzburg, A., Peters, D.A., and Hamilton, R.M. (1983).Crustal structure of the Northern Mississippi Embayment and a comparison with other continental rift zones, Tectonophsics, 94, 327−348.

Nelson, K.D., and Zhang, J. (1991). A COCORP deep reflection profile across the buried Reelfoot rift, south-central United States, Tectonophysics, 197, 271–293.

Nelson, W.J., and Lumm, D.K. (1985). The Ste. Genevieve Fault Zone, Missouri and Illinois, Illinois State Geological Survey Contract/Grant Report, 94.

Olive, W.W. (1972). Geology of the Jackson Purchase Region, Kentucky. Kentucky Geological Survey, 11.

Olive, W.W. (1980). Geologic maps of the Jackson Purchase Region, Kentucky. U.S. Geological Survey, Miscellaneous Investigations Series, Map I-1217, 11.

OYO Corporation. (2009). SeisImager Manual Version 3.3 [Computer program manual]: OYO Corporation.

Pryor, W.A. (1960). Cretaceous sedimentation in upper Mississippi Embayment, American Association of Petroleum Geologists Bulletin, 44, 1473–1504.

Russ, D.P. (1982). Style and significance of surface deformation in the vicinity of New Madrid, Missouri, in McKeown, F.A., and Pakiser, L.C., eds., Investigations of the New Madrid, Missouri, earthquake region, U.S. Geological Survey Professional Paper 1236-I, 95−114.

Rutledge, F. A., III. (2004). High-resolution geophysical investigation in the lower Wabash Valley Fault Zone. University of Kentucky, Lexington, Ky.

Slagstad, T., Culshaw, N.G., Daly, J.S., and Jamieson, R.A. (2009). Western Grenville Province holds key to Midcontinental Granite-Rhyolite Province enigma, Terra Nova, 21, 181-187.

Sexton J.L., and Jones, P.B. (1986). Evidence for recurrent faulting in the New Madrid Seismic Zone from Mini-Sosie high-resolution reflection data, Geophysics, 51, 1760−1788.

Soderberg, R.K., and Keller, G.R. (1981). Geophysical evidence for deep basin in western Kentucky, American Association of Petroleum Geologists Bulletin 65, 226-234.

Thomas, W.A. (1976). Evolution of the Ouachita-Appalachian continental margin, Journal of Geology, 84, 323-342.

Thomas, W.A. (1983). Continental margins, orogenic belts, and intracratonic structures, Geology, 11, 270-272.

Thomas, W.A. (1985) The Appalachian-Ouachita connection: Paleozoic orogenic belt at the southern margin of North America, Annual Review of Earth and Planetary Sciences, 13, 175–199.

Thomas, W.A. (1991). The Appalachian-Ouachita rifted margin of southeastern North America, Geological Society of America Bulletin, 103, 415–431.

Thomas, W.A. (2006). Tectonic inheritance at a continental margin, GSA Today, 16, 4-11.

Tollo, R., Aleinikoff, J., Borduas, E., Hackley, P., and Fanning, M. (2004). Petrologic and geochronologic evolution of the Grenville Orogen, northern Blue Ridge Province, Virginia. in Tollo, R., Corriveau, L., McLelland., Bartholomew, M. Proterozoic tectonic evolution of the Grenville orogen in North America, Geological Society of America Memoir, 197, 647–677.

Van Arsdale, R.B. (2009). Adventures through deep time: The Central Mississippi River Valley and its earthquakes, Geological Society of America Special Paper 455, 107.

Van Arsdale, R. B. and TenBrink, R.K. (2000). Late Cretaceous and Cenozoic geology of the New Madrid Seismic Zone, Bulletin of the Seismological Society of America, 90, 345-356.

Van Schmus, W.R., Bickford, M.E., and Turek, A. (1996). Proterozoic geology of the east-central Midcontinent basement. In van der Pluijm, B.A., and Caracosinos, P.A., eds., Basement and Basins of Eastern North America, Geological Society of America Special Papers, 308, 7–32.

Veezhinathan, J., and Wagner, D. (1990). A neural network approach to first break picking, International Joint Conference on Neural Networks Proceedings, 235–240.

Ventosa, S., LeRoy, S., Haurd, I., Pica, A., Rabeson, H., Ricarte, P., and Duval, L. (in press). Adaptive multiple subtraction with wavelet-based complex unary Wiener filters, Geophysics.

Wang, Z., and Woolery, E.W. (2006). Recordings from the deepest borehole in the New Madrid Seismic Zone, Seismological Research Letters, 77, 148−153.

Widess, M.B. (1973). How thin is a thin bed, Geophysics, 38, 1176-1180.

Woolery, E.W., and Street, R. (2002) Quaternary fault reactivation in the Fluorspar Area Fault Complex of western Kentucky–Evidence from shallow SH-wave reflection profiles, Seismological Research Letters, 73, 628–639.

Woolery, E.W., Schaefer, J., and Wang, Z. (2003). Elevated lateral stress in unlithified sediment, Midcontinent United States—Geotechnical and geophysical indicators for a tectonic origin, Tectonophysics, 368, 139–153.

Woolery, E.W., Street, R., Wang. Z., and Harris, J. B. (1993). Near-surface deformation in the New Madrid Seismic Zone as imaged by high-resolution SH-wave seismic methods, Geophysical Research Letters, 20, 1615-1618.

Yilmaz, Ö. (1991). Seismic data processing, Society of Exploration Geophysicists, Investigations in Geophysics, 2, 1-82.

VITA

- Born 2-15-1987 in Nashville, Tennessee
- University of Tennessee at Martin, Bachelors of Science: Geology
- Carrington Lee Wright